DEVELOPMENT AND VALIDATION OF TROMBE WALLS IN AUTODESK
SIMULATION CFD$^{\text{TM}}$

A Thesis
by
CHELSEA RENEE DAVIS

Submitted to the Graduate School
at Appalachian State University
in partial fulfillment of the requirements for the degree of
MASTER OF SCIENCE

May 2016
Department of Sustainable Technology and the Built Environment

DEVELOPMENT AND VALIDATION OF TROMBE WALLS IN AUTODESK
SIMULATION CFD^{TM}

A Thesis
by
CHELSEA RENEE DAVIS
May 2016

APPROVED BY:

_____

Jeffrey E. Ramsdell
Chairperson, Thesis Committee

_____

Andrew W. Windham
Member, Thesis Committee

_____

D. Jason Miller
Member, Thesis Committee

_____

R. Chadwick Everhart
Chairperson, Department of Sustainable Technology and the Built Environment

_____

Max C. Poole, Ph.D.
Dean, Cratis D. Williams School of Graduate Studies

Abstract

DEVELOPMENT AND VALIDATION OF TROMBE WALLS IN AUTODESK SIMULATION CFD™

Chelsea Renee Davis
B.S., North Carolina State University
M.S., Appalachian State University

Chairperson: Dr. Jeffrey Ramsdell

Computational Fluid Dynamics (CFD), as an architectural tool, has the potential to model the air flow and convective heat transfer that predominates the performance of passive solar building techniques to meet the comfort needs of building occupants; however, there is very little research on the implementation or validation of CFD software for this purpose. This study attempts to validate a verified CFD software program, Autodesk CFD, for the purpose of modeling both unvented and vented Trombe walls. Temperature and air velocity data from two past experimental studies were compared to model results. The results indicate that CFD may be used to simulate and visualize buoyancy driven air flow and mass wall heat transfer closely resembling actual Trombe walls. This study also shows that accuracy and computational time of simulations are largely dependent on user defined input such as time step size. Further research into validation and creation of optimization workflow protocols using Autodesk CFD for Trombe wall design is recommended.

Table of Contents

List of Tables

List of Figures

Chapter One: Introduction

As recently as 2014, approximately 35% of residential and commercial building energy use in the United States was used for mechanical heating, ventilation, and air conditioning (HVAC) systems (Energy Information Administration, 2014). The climate, geometry, materials, and occupant use of the building determines the amount of mechanical assistance needed to meet the comfort needs. Mechanical HVAC systems require a source of energy, electricity or burning fuel, to provide thermal comfort and acceptable indoor air quality. Passive solar building techniques effectively collect, store, and distribute solar energy to provide thermal comfort without the need of electricity or burning fuel. Sunspaces, direct gain walls, and Trombe walls are all passive solar techniques. These replace standard insulated walls and are composed of different arrangements of glazing and materials of high thermal storage capacity. The use of passive solar building techniques reduces the thermal load on mechanical HVAC systems which decreases energy consumption and demand (Balcomb, 1992).

The Trombe wall system is a passive solar building technique that uses a mass wall, glazing, vents, and dampers in different configurations to aid in heating or cooling the home. Figure 1 shows a diagram of both heating and cooling Trombe wall configurations. In the summer, the Trombe wall acts as a solar chimney by drawing air from the building, through the buoyancy effect, and producing a natural breeze through the home. In the winter, the dampers of the Trombe wall can be adjusted to create warm convective currents within the cavity wall. Those currents are then distributed throughout the building along with radiated heat from the mass wall. This study will focus on Trombe walls configured for winter heating. The incorporation of a Trombe wall has been shown to reduce overall energy usage

in single-family residential buildings by 30% (Saadatian, Sopian, Lim, Asim, & Sulaiman, 2012, p. 6341).
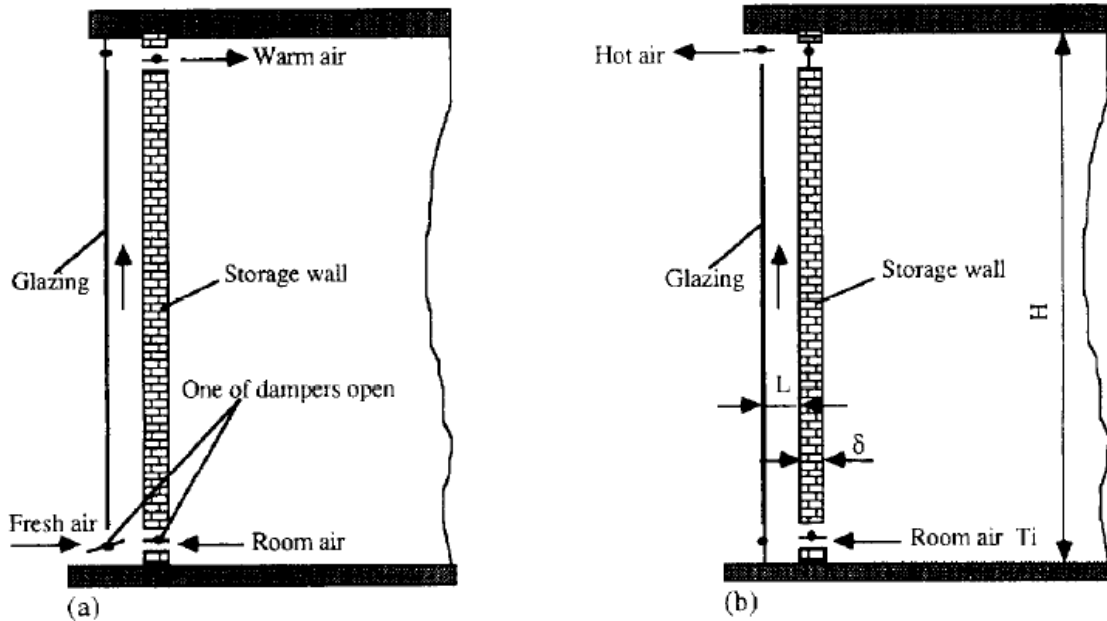
Figure 1. Schematic diagram of classic Trombe wall (a) winter heating, (b) summer cooling (Gan, 1998, p. 37).

A variety of methods has been used in an attempt to optimize Trombe wall design. Gan (1998) performed a parametric study using two-dimensional air flow measurements for different wall heights, glazing types, and wall insulation to optimize the cooling effects of a Trombe wall. Simplified sets of the Navier-Stokes equation have been used to calculate the heat transfer, fluid flow, and fluid temperature profile within the cavity wall (Zamora & Kaiser, 2009). Although these studies have assisted in producing a range of design criteria for certain aspects of Trombe walls, there are many assumptions used to reduce the complexity of the simultaneous partial derivative flow equations needed to analyze such a complex system. This makes numerical analysis difficult to use as a design tool unless it is housed in a more capable computational package. Similarly, experimental works are limited by time and

2

cost in the amount of variables that are able to be tested. The use of a simulation software

that incorporates verified Computational Fluid Dynamics (CFD) code would allow for

multiple parameters to be tested and optimized in various climates if it can be validated with

existing experimental data. Validation involves the comparison of experimental data to the

results of a simulated model; validation and verification of simulation software for a

particular use creates confidence in the software to be used as a design tool.

Statement of the Problem

Simulation of a digital prototype can be useful in the design and optimization of any

product. The simulation of a building may be used to review and reduce energy use, identify

costly conflict before construction, and optimize user comfort. Energy use as an optimization

metric does not pertain to the design of a completely passive building. When designing

buildings that incorporate both active and passive systems, energy use is still an important

metric; however, the level of thermal comfort provided by the passive system must be known

to know how much energy is offset from the active system. The comfort performance of a

passive heating or cooling system cannot adequately be quantified in a building energy

modeling program that does not account for air flow and convective heat transfer within the

air space of the building.

Building Energy Simulation (BES) tools possess many shortcomings when it comes to

modeling passive solar building systems. One of the primary drawbacks of BES is its

inaccuracy when calculating heat transfer by convective currents (Haupt, Kunz, Paltier, &

Dreyer, 2010; Ellis, 2003). Table 1 shows the difference between BES and CFD software as

far as capabilities in building simulation.

3

Table 1

Comparison of BES and CFD Simulation (AbdElrahman & ElDabosy, 2013, p. 5)

Building performance study	ES	CFD
Weather and solar impact	Yes	No
Enclosed thermal behaviors	Yes	No
HVAC system capacity	Yes	No
Energy consumption	Yes	No
Thermal comfort (air temperature, air velocity, relative humidity and airflow turbulence)	No	Yes
Indoor air quality (contaminant concentrations)	No	Yes
Air distribution	No	Yes

CFD allows designers to simulate and visualize the distribution of temperature, air velocity, the concentration of water vapor and contaminants, thereby allowing optimization of occupant comfort and health in the building. Building ventilation performance and indoor air quality studies have validated CFD code to experimental data with good results (Chen, 2009). A combination of grid generating (GRIDGEN), heat transfer (RadTherm), and computational fluid dynamics software (nPhase) were used to model a Trombe wall in the design phase of a commercial building (Sami & Gassman, 2006). The building was not monitored to validate the results of the combined software. Validation studies and studies that test workflow processes using various CFD tools will help to further the use of CFD in both Trombe wall specific, and overall building design.

Purpose of the Study

There are three methods to approach a heat transfer or fluid dynamic problem: experimentally, theoretically, or computationally. The Trombe wall is an excellent combination of both a fluid dynamic and heat transfer problem that has been extensively

studied using the former two approaches. From these studies, multiple design guidelines have been created. Unfortunately, experimental studies are building and climate dependent while theoretical studies are restricted to simple geometry and physics. This limits the effectiveness and accuracy of the current design guidelines. The goal of this research is to validate Autodesk CFD for use with Trombe walls by modeling and comparing the results to past experimental test modules. An Autodesk product was chosen due to the interconnectivity of CAD, BIM, and BES tools that are frequently used in architecture and engineering firms. Designs created in Autodesk Revit are transferable to both the CFD tool and the BES tool, Ecotect.

The aim of this study is to simulate existing Trombe wall test cells described in (Casperson & Hocevar, 1979; McFarland, 1982) to provide confidence in using Autodesk CFD for the custom design of Trombe walls. An anticipated result of this study is a workflow process for creating and testing Trombe walls, and similar thermal storage wall systems, using CFD software. This process will involve three main components: (1) the creation of a model workflow, (2) an analysis method for simulation outputs, and (3) a sensitivity analysis of time steps and mesh sizes. An additional purpose of this study is to advance the incorporation of CFD simulation in building design and of Trombe walls in passive solar design.

Research Questions

These questions are designed to analyze the chosen software, Autodesk CFD 2016, in its ability to model the complex air flow and heat patterns within a Trombe wall test cell.

1. Does a buoyant driven air flow pattern exist in the visualization of the vented Trombe wall simulation results?

2. How similar are simulated outputs of temperature and air velocity to measured outputs of past experimental studies? Do these outputs change as expected with differences in Trombe wall configuration?

3. How does variance in the numerical scheme of the simulation affect accuracy?

Limitations of the Study

The use of computer simulation in any research introduces a risk of user error due to lack of background knowledge or due to incomplete input information. A general knowledge of fluid dynamics, heat transfer, and numerical methods is needed to make informed inputs into the simulation software. This limitation may be counterbalanced through the use of verification methods such as comparison of results to numerical analyses or to actual model results. Incorrect settings of boundary conditions, grid resolutions, numeric techniques, and interior heat sources can attribute to differences from measured data. ASHRAE's procedure for verification, validation, and reporting of indoor environment CFD analyses provides a guideline for these settings (Chen & Srebric, 2002).

Another limitation of the study is the availability and accuracy of experimental data. Some climate conditions and material properties were not reported in these studies. It must also be assumed that all the reported sensor data is correct and accurate. Unknown material properties can be estimated based on similar materials. Unknown conditions like infiltration will not be accounted for in the study but may contribute to result uncertainty. The reported error range of the sensors will be considered in the analysis of model data accuracy. There

have not been many recent experimental studies regarding Trombe walls so this validation

will need to rely on the accuracy of data collected from the few past experimental and

numerical studies.

Significance of the Study

The use of computer simulation is used in optimizing and testing building designs

before construction to reduce risk and construction cost. The use of computer simulation tools

also enables the testing of innovate design techniques such as the incorporation of new

materials and geometries that would be too costly to test experimentally. Computational fluid

dynamics is theoretically more capable of quantifying and designing a passive system than

building energy simulating software. This study will help reveal the capabilities of Autodesk

CFD for use in simulating Trombe walls. In attempting to validate the software for this purpose

a workflow process will be created and tested. This workflow process may be referenced by

those wishing to use CFD for the design of similar building devices.

The simulation tool, Autodesk CFD 2016, will be analyzed for its ability to

qualitatively depict air flow patterns and quantitatively predict temperature and air velocity at

certain points within the interior. If there is an agreement to the reference experimental

studies, then this work will serve as the foundation of a design optimization procedure. If

there is little agreement due to uncertainty the researcher suggests further research using

experimental studies designed for the purpose of validation.

Chapter Two: Review of Literature and Relevant Research

The History and Function of Trombe Walls

A Trombe wall system is a type of thermal mass storage wall that incorporates exterior glazing, vents, and dampers in order to passively heat, cool, and ventilate an interior space, depending on configuration (Hordeski, 2004). The Trombe wall shares a name with one of the French inventors who patented and popularized the architectural features, Felix Trombe and Jacques Michel (1972). Figure 1 shows the original configuration of a Trombe wall for both heating and cooling. During the winter months, air enters the cavity from a low vent. The air is heated up by the wall and rises through the cavity and into the room through the buoyancy or stack effect. During warm summer months, the Trombe wall can act similarly to a solar chimney by closing the low glazing vent and opening the high vent (Gan, 1998). Instead of utilizing the buoyancy effect within the cavity to push heated air into the living space the summer configuration will pull air from across the room, through the cavity, and out an external vent, which will create cooling ventilation and remove warm air.

Experimental and numerical studies have been done to generate a set of guidelines for Trombe wall design. Some general Trombe wall design guidelines include a suggested mass wall thickness of between 10-16 inches and a cavity of between 1 and 2.5 inches (Wilson, 1979). The mass wall of the Trombe wall system is most commonly a dark colored and south-facing (Northern Hemisphere) concrete, masonry, or earthen wall. The mass wall portion of the system serves to collect and store solar energy during the day and release this heat energy when needed. While these guidelines provide a general framework for a workable Trombe wall they are neither climate specific nor specific to the needs of the

8

individual building. A validated simulation technique would enable these guidelines to be tested and optimized for specific climates and building uses.

Review of Research on Trombe Walls

Trombe walls incorporate various accessories including vents, dampers, and fans to achieve efficiency given different exterior conditions. Studies of the optimal placement, dimensions, and operations of these accessories are the predominant experiments done on optimization of Trombe wall system (Saadatian et al., 2012; Kim & Seo, 2012; Zamora & Kaiser, 2009). A study looking specifically at thermo-circulation vents, one vent at the top and one at the bottom of the mass wall, showed that the closing of vents at night and when the internal temperature exceeded 24° C would avoid creating a reverse flow or overheating, respectively (Saadatian et al., 2012, p. 6346). Additionally, studies have shown the addition of external vents as well as the size and distance between mass wall vents have a significant effect on air circulation (Kim & Seo, 2012). Kim & Seo performed an experimental study mixed with 2-D CFD simulation to measure air flows based on vent spacing. An optimal distance that minimized heat loss without compromising air flow was found around 1.5 meters. This configuration did not factor in differing vent opening areas or varying air gap thicknesses. A parametric study of Trombe walls for passive cooling using turbulence models and a review of past experimental studies showed ventilation rates increase with air gap thickness and when using double-paned glazing instead of single-paned (Gan, 1998). This study also suggested that the interior surface of the mass wall be insulated to prevent overheating due to radiation.

A collection of literature on Trombe walls done by Saadation et al. (2012) shows that the mass wall's thickness, the air gap thickness, and vent sizing and spacing have the most drastic effect on Trombe walls. The optimal thickness of the mass wall is dependent on the thermal capacity of the materials chosen, on climate, and on the shape and function of the connected livable space. The mass wall of a classic Trombe wall is composed of materials of high heat storage capacity including bricks, concrete, stone, or adobe. Some modern Trombe walls are using lighter water walls and phase change materials in place of masonry. The experimental test cells referenced in this study used concrete mass walls. Concrete has a thermal lag of 120 to 150 minutes for every four inches of thickness. Too thin of a mass wall will result in excessive interior temperature swings while too thick of a mass wall will be costly to build and will take too long to radiate heat into the interior after peak exposure, creating occupant discomfort. The optimal suggested mass wall thickness proposed is between 30 and 40 cm (11.8 to 15.7 inches).

Zamora and Kaiser (2009) used two-dimensional laminar and turbulent numerical models, along with experimental models, for different geometric configurations of the Trombe wall. The Nusselt number and the calculated mass flow rate were used as indications of effectiveness. The total energy flow can be found by multiplying the Nusselt number by the mass flow rate. This study concluded that the ratio of air gap thickness to wall height was far more significant than the ratio of vent size or wall thickness to wall height. A further look into the numerical methods involved in analyzing the natural convective currents and heat transfer within a Trombe wall will be discussed in a later section.

Experimental Studies of Vented and Unvented Trombe Walls

Because the use of CFD in building system design has only recently gained a foothold through indoor building environment studies, there are very few precedents upon which to base a validation method. Validation involves demonstrating the ability of a user and a CFD code to accurately simulate a representative environment. For most computer simulation software the best way to legitimize simulated values is to compare with actual monitored values of the exact same configuration as the model (Chen & Srebric, 2002). In order for an experimental study to qualify as a source of comparison, the space must be monitored, controlled, and be free of confounding variables such as unmeasured mechanical HVAC or occupant use.

Two different experimental studies were chosen to model in Autodesk CFD based on configuration and available data. The experimental models used are 3 unvented Trombe wall test cells in Los Alamos, NM (McFarland, 1982) and 3 configurations of a vented Trombe wall in Idaho Springs, CO (Casperson & Hocevar, 1979). Both of the selected experimental studies were performed in the late 1970's and early 1980's. Additional Trombe wall experimental studies are included in this literature review but were not selected due to either a lack of accessible data or an overabundance of confounding variables.

The most notable set of passive system test cells is located at the Los Alamos National Laboratory (LANL) in New Mexico (Ellis, 2003). This study was composed of 14 test cells with various passive heating techniques, four of which incorporate a type of unvented Trombe wall. These test cells have been monitored since 1980 by an increasingly complex data acquisition system. Many studies involving Trombe walls have used the Los Alamos test cells as a means of calibration and verification of results (Gan, 1998; Ellis,

2003). Due to limited reported cell data and local climate data, only eight consecutive days in the winter of 1982 were used for simulating.

Vented systems would be more indicative of the CFD capabilities to simulate buoyancy driven air flow to the interior space. The NREL Wind Site in Colorado has a 44 ft^2 vented Trombe wall on the southern wall with a single-paned low-iron glazing over a 4-inch mass wall (Ault, Torcellini, & Van Geet, 2003). The visitor center at Zion National Park in Utah is another vented Trombe wall that has been reported on and measured (Torcellini & Pless, 2004). This design is composed of a 6-foot-high Trombe wall with a total area of 740 ft^2 on the southern wall. The wall is composed of 8 inches of grout-filled concrete masonry units and a single piece of high transmittance patterned glass with a 2-inch air gap between. A high-set window within the mass wall is used as the inlet vent. This facility has been monitored for interior temperature and humidity for two full years. The large square footage and frequent occupancy of the visitor center would make it difficult to attribute the variations in temperature and humidity to the Trombe wall system.

The vented experimental study was selected based on the availability of reported data and simplicity of geometry. This study was performed by Richard L. Casperson and Carl J. Hocevar of Energy Engineering Group, Inc. in Idaho Springs, Colorado as part of a U.S. Department of Energy contract. One test facility with three different configurable air gap thickness was tested. Temperature and air velocity were tested at 15-minute intervals throughout the air gap. While the test cell was monitored from January to April of 1979 only data from 10 selected clear sky days were reported (Casperson & Hocevar, 1979). Both selected studies only had available data from winter conditions so the validation could only be performed for heating capabilities.

Numerical Analyses of Trombe Walls

Numerical analyses have been used in an attempt to optimize the design of Trombe walls (Zamora & Kaiser, 2009). The governing equations (Navier-Stokes Equation is shown below) dictating the convective heat transfer and air flow within a system are derived from the fundamental laws of mass, energy, and momentum conservation.

Equation 1, Simplified Navier-Stokes Equation (Chen & Srebric, 2002, p. 2).

$$\frac{\partial}{\partial t}(\rho\phi) + \frac{\partial}{\partial x_j}(\rho U_j \phi) = \frac{\partial}{\partial x_j}\left(\Gamma_\phi \frac{\partial\phi}{\partial x_j}\right) + S_\phi$$

Transient + Convection = Diffusion + Source

Each section of the equation represents a change over time of air velocity, temperature, or species concentration in a three-dimensional space. These coupled partial derivations can be solved algebraically if the geometry is divided into smaller control elements or volumes. The finer the volume discretization the more computationally intensive. Computer-based numerical procedures are the only practical means of generating complete solutions to these equations. CFD simulations utilize the governing equations to simulate the interaction of fluid flow with surfaces of finite volumes or elements defined by boundary conditions.

Simplified sets of the Navier-Stokes model can be used if assumptions are made for incompressible and inviscid flows. Manz and Frank (2005) looked at airflow patterns within a double-skinned façade and found turbulent flow (high Reynolds number) can be assumed for a majority of cases. Based on this assumption the k-ε turbulence model for recirculating flows can be used to some degree of confidence as shown by Zamora and Kaiser (2009). From an assumed high Reynolds and Rayleigh number the ratio of convective to conductive heat transfer can be assumed to be high as well, which enables an approximation of the

13

Nusselt number by dividing the local heat transfer coefficient (h) and the height of the wall (H) by the thermal conductivity of air (k). These assumptions can be verified by a CFD simulation, or by comparison to experimental results of a built system. These numerical studies also give an idea of what turbulence model to select in the CFD tool. Autodesk CFD gives the option of using k-epsilon, renormalized group (RNG), or low Reynolds k-epsilon.

The Use of Computational Fluid Dynamics in Building Science

CFD is used to model the behavior of fluids. For building science purposes this will mainly relate to the movement and temperature of air within a space (Zhai, 2006). CFD software uses the general equations of energy, mass, and momentum conservation to calculate the transfer of mass and heat between discretized volumes. The air movement, air temperature, and radiant temperature of the boundaries of these volumes are set to a starting condition. These boundary conditions are based on local climate or material data. Once the boundary conditions are set the CFD software will then simulate the flow of air and exchange of heat from the boundary surfaces to the adjacent volumes then to each volumes surrounding.

A CFD code solves the heat flow and transfer models by dividing the continuous space into finite elements or volumes (Chen & Srebric, 2002). The space can be divided into structured or unstructured numerical grids. Structured mesh grids are based on Cartesian coordinates and are for uncomplicated rectangular volumes. Unstructured meshes are body-fitted and better when complicated or curved surfaces exist. Unstructured meshes more accurately simulate heat transfer between the human body and the surrounding air. The experimental Trombe walls referenced in this study are not occupied, nor do they contain any

curved geometry. For the purpose of comfort performance measurement and custom Trombe wall design in further research; however, an unstructured mesh would be necessary. For this reason, CFD software that is able to develop body-fitted and curved surface mesh is preferable.

Where CFD is being used to predict user comfort, it is important that both air temperature and radiant temperature are considered. Typically, CFD itself only models air temperature and fluid velocity. The Autodesk CFD tool is able to include radiant influences on the temperatures that will be felt and produced by occupants. In Autodesk CFD, a thermal mannequin can be set up to mimic the metabolic and radiant heat generated by a person while also serving as a monitor point for comfort conditions.

Review of relevant computational fluid dynamic studies.

The application of CFD simulation has been validated with numerical models of indoor air quality, mechanical ventilation, and stratified ventilation within buildings (Chen, 2009)**.** The integration of CFD simulation into building design optimization has been used in projects requiring a high degree of precision in ventilation systems such as in hospitals and server rooms or in high-rise site planning to reduce high-speed wind between buildings (Zhai, 2006; Chen, 2009). There is a variety of software used and a variety of methods. From the following articles, it can be shown that CFD is effective in simulating air flow and heat transfer in buildings.

CFD coupled with building energy simulation has been used to design natural ventilation systems and double-skinned facades in office buildings (Abdelrahman & ElDabosy, 2013; Manz & Frank, 2005). Two-dimensional CFD along with experimental analysis was used to show the air flow distribution in a room with a chilled ceiling (Catalina,

Virgone, & Kuzink, 2009). FloVent, a three-dimensional CFD that specializes in HVAC applications, was used to analyze cooling towers in four different climate conditions (Sami, 2003). There have been CFD studies that analyze pre-existing Trombe walls using a combination of software to create the mesh and to run the calculations using Radtherm with nPhase (Sami & Gassman, 2006). This study, in particular, was conducted to display the temperature and air flow gradient along a Trombe wall in Asheville, NC throughout the year. Comparing this with actual energy and interior temperature data it was shown that the Trombe wall was potentially saving the Blue Ridge Visitor Center 128.5 million BTU/year or 35% of the building's space heating load (p. 11). This study showed that Trombe walls can be analyzed using methods that are similar to a full CFD software package. There were no reported studies, to the researcher's knowledge, that used Autodesk CFD to model a thermal storage mass wall or compared the results of a Trombe wall modeled using a CFD tool to experimental data.

Procedure for validation of CFD analyses.

Validation of a simulation program involves a demonstration of the user's ability to accurately replicate a phenomenon for which reliable data exists. The procedure and criteria necessary for validating CFD analyses to indoor environmental applications were investigated and reported on by ASHRAE members, Chen and Sreberic (2002). The level of accuracy reported in validation to a specific application, such as a pre-existing Trombe wall, determines the level of confidence in using the program for future design purposes. The procedure suggested involves matching the geometry and initial conditions as close as possible to the experimental study, running an isothermal flow analysis, and then adding heat transfer. These suggestions are considered in the methodology of this research study.

Chapter Three: Methodology

This study focuses on the capability of Autodesk's CFD tool and the user to simulate the complex heat transfer and convective flow patterns within Trombe walls by comparing modeled results to experimental study results. The experimental studies chosen include three unvented test cells from the Los Alamos Passive Solar study (McFarland, 1982) and three vented test cell configurations from Idaho Springs, Colorado (Casperson & Hocevar, 1979). The Las Alamos National Lab (LANL) test cells were monitored hourly, primarily during winter months, between 1979 and 1982. The sensors installed within the LANL cells monitored for temperature at various locations within the cell. Accessibility to both monitored cell data and weather data within these three years narrows the time frame used in this study to between February 14 and February 22, 1982. Congruent data spanning multiple days will help gauge the ability of the software to predict the diurnal patterns of heat storage expected from a system that incorporates a thermal mass.

The Energy Engineering Group (EEG) at Golden, Colorado test cell configurations were tested in the winter months, January and February, in 1979. Data was reported for two clear sky days for two, four, and six-inch air gaps. The EEG cell was monitored for temperature of the mass wall and glazing as well as the velocity of air within the air gap.

The steps in the workflow of Autodesk's CFD tool include the following in chronological order; create geometry, define materials, define boundary conditions and initial environment, create a mesh, set solving parameters, then solve and analyze results. All simulations were run on an ASUS K501 laptop with a Dual-Core Pentium CPU @ 2.30 GHz processor with an installed memory (RAM) of 4GB.

Creating Geometry

The geometry was created using Autodesk Revit 2015 and then exported as a Standard ACIS Text (SAT) file to create a design study in Autodesk CFD 2016. For the purpose of properly simulating heat transfer between elements of the construction, all walls, roofs, and floors were split into parts by material type before exporting. This would also ensure that material properties were properly accounted for. While both studies had wood stud and joist systems these components were not accounted for separately in either model. The conduction through the insulated portion of the wall, roof, and floor system was not the primary focus of this study and could be represented by an averaged reported conductivity.

Complex geometry such as door and window frames were removed from the model and accounted for in material properties or substituted with simplified geometry. An overly detailed model would require more mesh elements which would result in a longer computational time. It is also important to make sure there are no overlapping geometry or small gaps prior to exporting. Once in the CFD program, the mesh diagnostic tool was used to identify possible edges and surfaces that could cause errors. The geometry tools in Autodesk CFD were used to fill voids with volumes and to create an external volume around the model. Both these volumes would later be defined as air.

The dimensions of the geometry used were based on descriptions and figures from the experimental study reports (McFarland, 1982; Casperson & Hocevar, 1979). Any dimensions that were not reported in the original report were assumed based on derived research that has used the Los Alamos test cells for numerical and building energy modeling validation (Ellis, 2003).

Los Alamos test cells.

Los Alamos National Lab's passive solar study consisted of 14 paired test cells. The layout of the 14 test cells as well as a description of the passive heating techniques can be seen in Figure 2. Cells 1, 2, and 12 include Trombe walls and are investigated in this study. Cell 11 is included in the study to account for the changing conditions of the interior wall of cell 12. Cell 13 is included to replicate the shading of cell 12. All test cells are facing true south within 0.5° (McFarland, 1982). The paired cells are spaced approximately 1.4 meters apart or 54 inches based on photographic scaling (Ellis, 2003). Figure 3 shows the geometry of a standard test cell from this study.
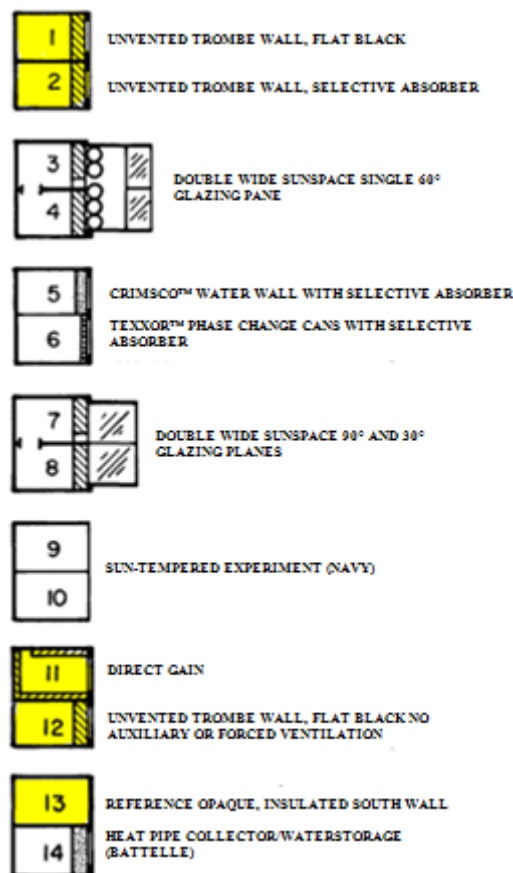
Figure 2. Los Alamos test cell layout, modeled cells highlighted (McFarland, 1982, p. 7)
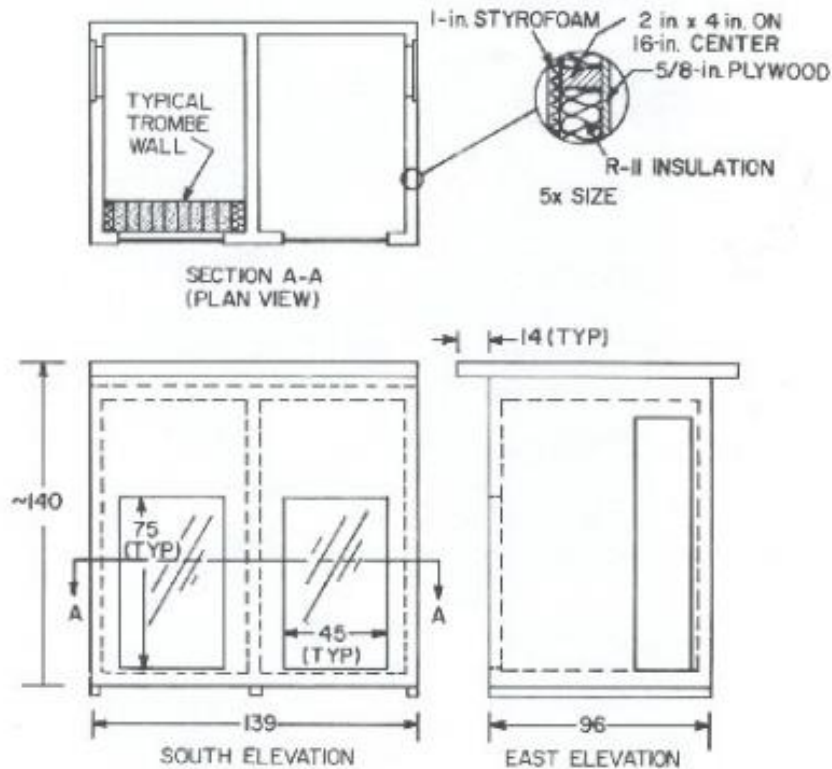
Figure 3. Los Alamos Passive Solar study test cell geometry (Ellis, 2003, p. 36).

The interior dimensions of each cell are approximately 120 in. high, 86 in. deep, and 62 in. wide (McFarland, 1982). There is a 2 ft. by 9 ft. access door to each cell made of 4 in. Styrofoam and 5/8 in. plywood on the exterior. The exterior walls are composed of 1 in. Styrofoam on the interior, 3 ½ in. wood studs with fiberglass batt insulation, and 5/8 plywood on the exterior. The interior walls are 3 ½ in. wood studs with fiberglass batt insulation surrounded by 1 in. Styrofoam. The mass walls are made of standard solid concrete masonry unit blocks measuring 5-5/8 in. by 7-5/8 in. by 15 5/8 in and extend the height of the interior. The glazing is 45 in. by 75. and is composed of 2 panes of 3/16 in. glass with ½ in. air gap. An air gap of 3 3/8 inch was used, creating a distance of 4 ¼

between the mass wall and the exterior of the glazing. Figures 4 and 5 show the created cell geometry and layout in relation to one another.

Figure 4. Plan view of unvented test cells modeled in Revit.
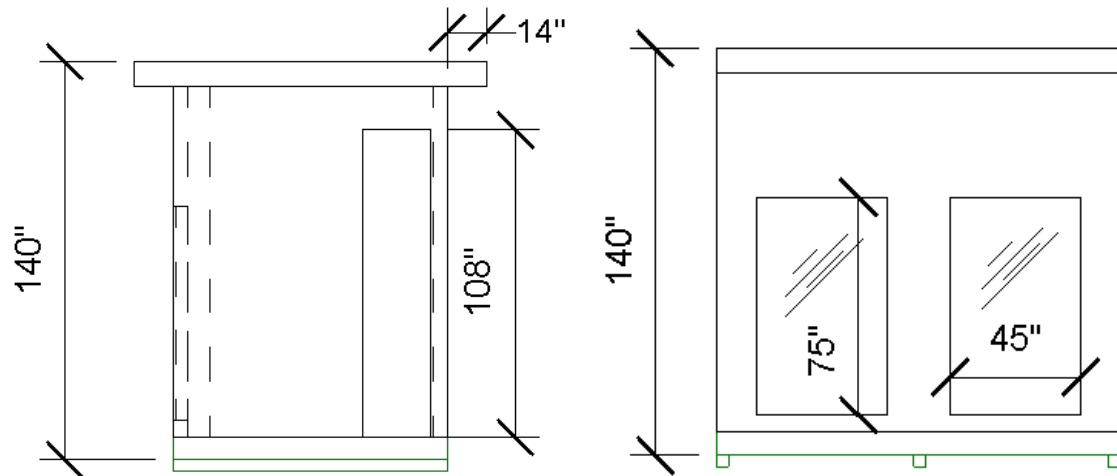
Figure 5. South Elevation (right) and East Elevation (left) of unvented test cells.

Given the distance between neighboring test cells, shading must be accounted for in the model. Shading is also provided by 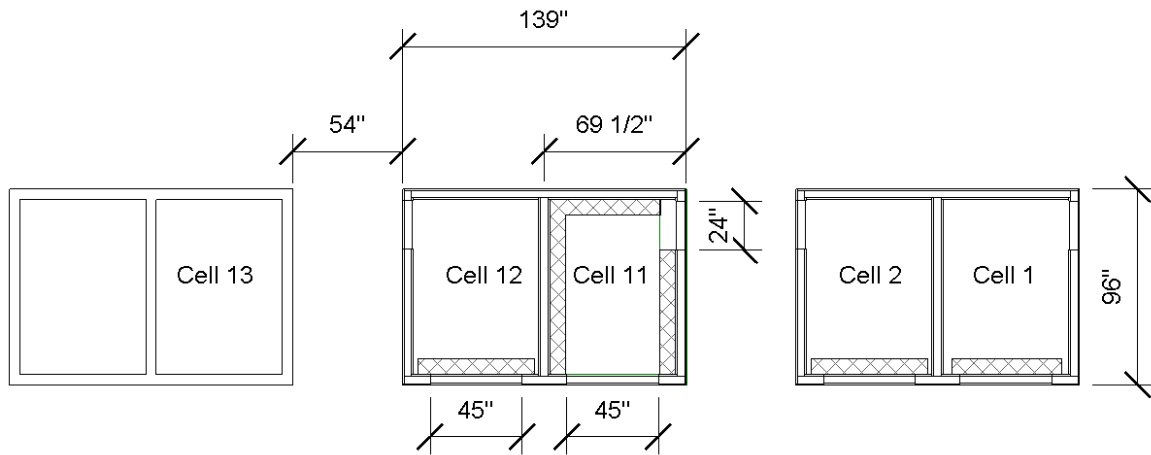the 14 in. roof overhang of the north and south side. Figure 6 is a 3D view of the modeled test cell with noon shading on the first day of acquired

measured data. The environment beyond the test cells may contribute to the shading but is not mentioned in the referenced reports.
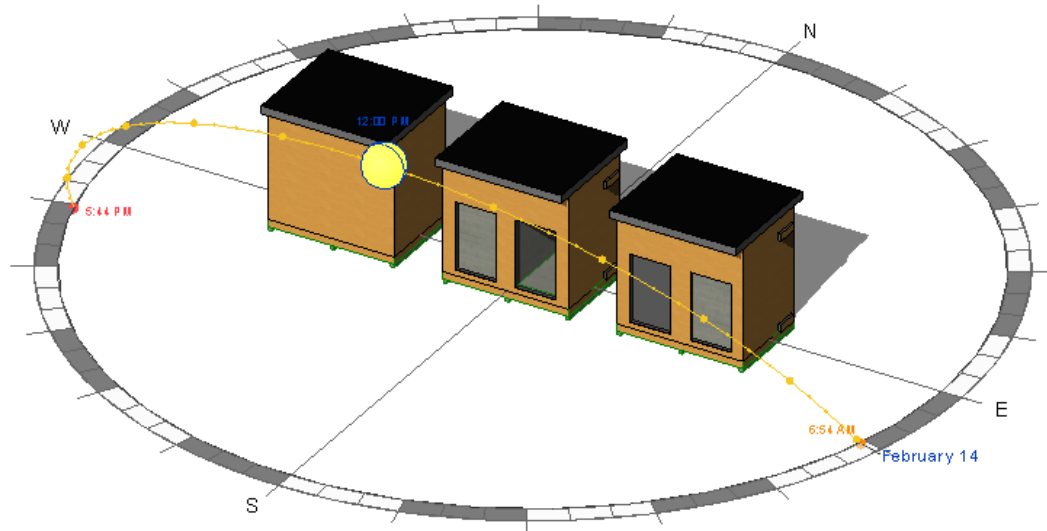
Figure 6. 3D View with Revit solar shade analysis.

The ceiling of the cells was constructed of 2 x 6 in. wood joists with two layers of 3 ½ in. batt insulation with 1/16 in. corrugated metal interior. The roof is 10 in. above the ceiling and is constructed of 90 lb. rolled roofing on 30 lb. felt on 5/8 in. plywood on 2 x 4 in. rafters. The floor is 2 x 6 joists with two layers of batt insulation surrounded by ¼ in. plywood facing on the interior and 5/8 in. plywood on the exterior. Risers were placed on the underside of each test cell to reduce conduction from the ground. The dimensions of these risers were not given but were assumed to be 4 x 4 wood pieces.

Other geometry elements to consider in the Los Alamos study are those of interior lighting and fans. The interior temperature of the Los Alamos cells was regulated using the auxiliary heat of a lightbulb in cells 1 and 2 of the modeled cells. Small centrifugal blowers

were used to regulate infiltration rates of 3 nominal air changes per hour. The specifics on the power output of the auxiliary heat and flow rate of the fan are specified later in the methodology. The fan and lighting geometry were too complex for the purpose of this study; simplified components were substituted. A 4 in. by 4 in. by 9 in. rectangle hanging from the center of the ceiling of cells 1, 2, and 11 were created to represent the light fixture. These same cells also included an 8 in. by 15 in. volume bridging between the interior and exterior wall surfaces to represent the installed centrifugal fan. The fan volume was extruded 4 inches from the surrounding exterior walls to allow the incoming air flow to stabilize before entering the interior space. The fan component was centered above the door. Cell 12 had neither auxiliary heating by lighting or fan forced ventilation no substitute geometry was required.

Energy Engineering Group test cell.

The vented experimental study, performed by Energy Engineering Group in Golden, Colorado, was composed of one configurable test cell (Casperson & Hocevar, 1979). The report did not include mention of any adjacent structures that would cast shade on the cell. The gap between the glazing and the mass wall was tested at 2 inches, 4 inches, and 6 inches from the masonry wall. Figure 7 shows the geometry of the test cell from the report. Figure 8 shows the geometry created in Revit.
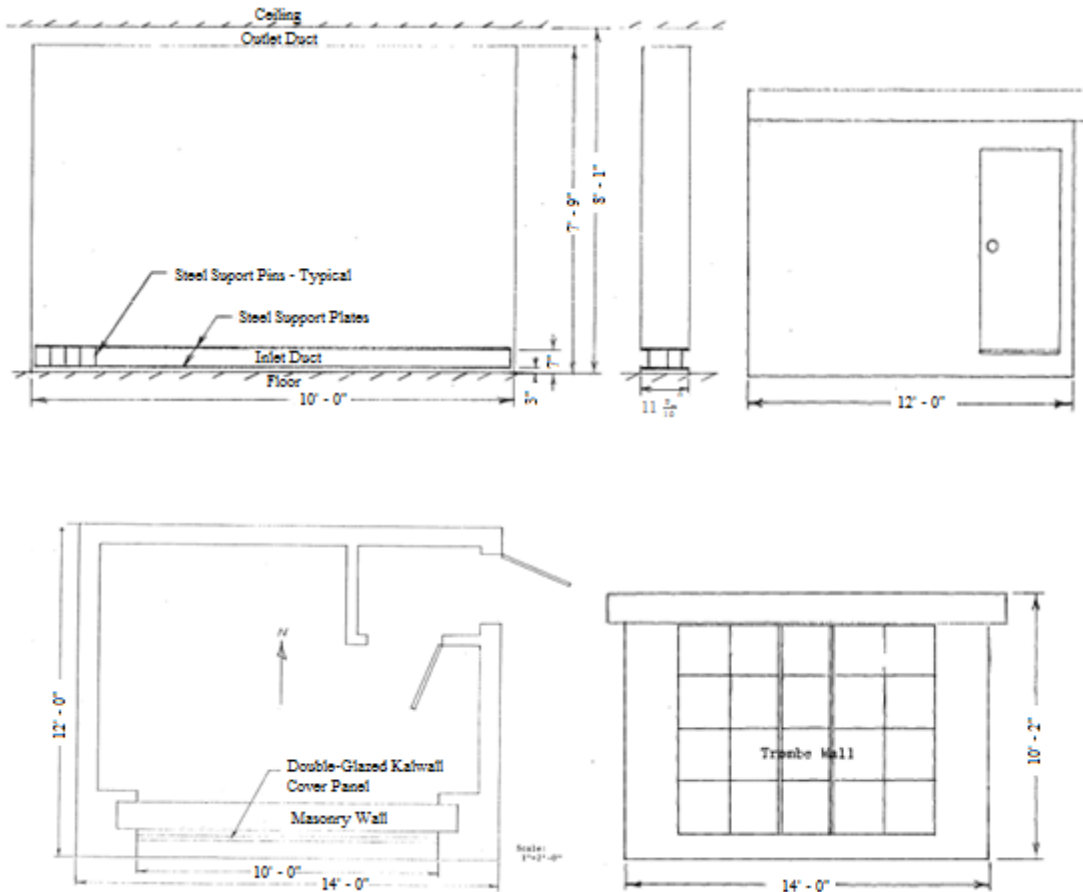
Figure 7. EEG vented study test cell geometry (Casperson & Hocevar, 1979 pp. 18-19).

The exterior walls are composed of ½ in. gypsum wallboard on the interior, 3 ½ in. wood studs, and ½ in. plywood on the exterior. The interior walls are uninsulated 3 ½ in. wood studs surrounded by ½ in. gypsum wallboard. The roof was constructed of 2 x 12 in. wood joists with a 3-ply asphalt built-up roof, the interior was ½ in gypsum. The floor is composed of 2 x 10 joists with ¾ plywood and linoleum covering. Tightly packed cellulose insulation was blown in under pressure for the exterior walls, roof, and floor system. Door were ¾ in. hollow core wood.

The mass wall was made of solid concrete masonry unit blocks measuring 7 5/8 in. high, 11 9/16 in. deep, and 15 9/16 in. wide. A 4 in. high gap extending the full 10 ft. length of the masonry wall between the top of the wall and the ceiling served as the outlet duct. A similarly sized gap between the bottom of the masonry wall and the floor served as the inlet gap. Steel pins attached to plates spanned the 4-inch ducts to support the mass wall and roof. The pins were determined to be of a negligible width to disrupt the inlet and outlet air flow so were not included in the geometry of the model. The glazing was fixed in a movable frame to adjust the gap from the mass wall between 2 inches, 4 inches, and 6 inches. The glazing was composed of two Kalwall panels separated by 1 ½ inch interior air film.

Additional geometry.

For both models, a ground volume was created in Revit to account for the heat transfer through the floor and the reflected solar radiation. The ground volume was three feet thick and had a diameter of 100 feet for both models. A ground volume of at least five times the width of the test cell was suggested (*Solar Heating*, 2016). Figure 9 shows the three-dimensional view of the vented model with the ground volume. The ground volume created for the Los Alamos cells can be seen in Figure 10.
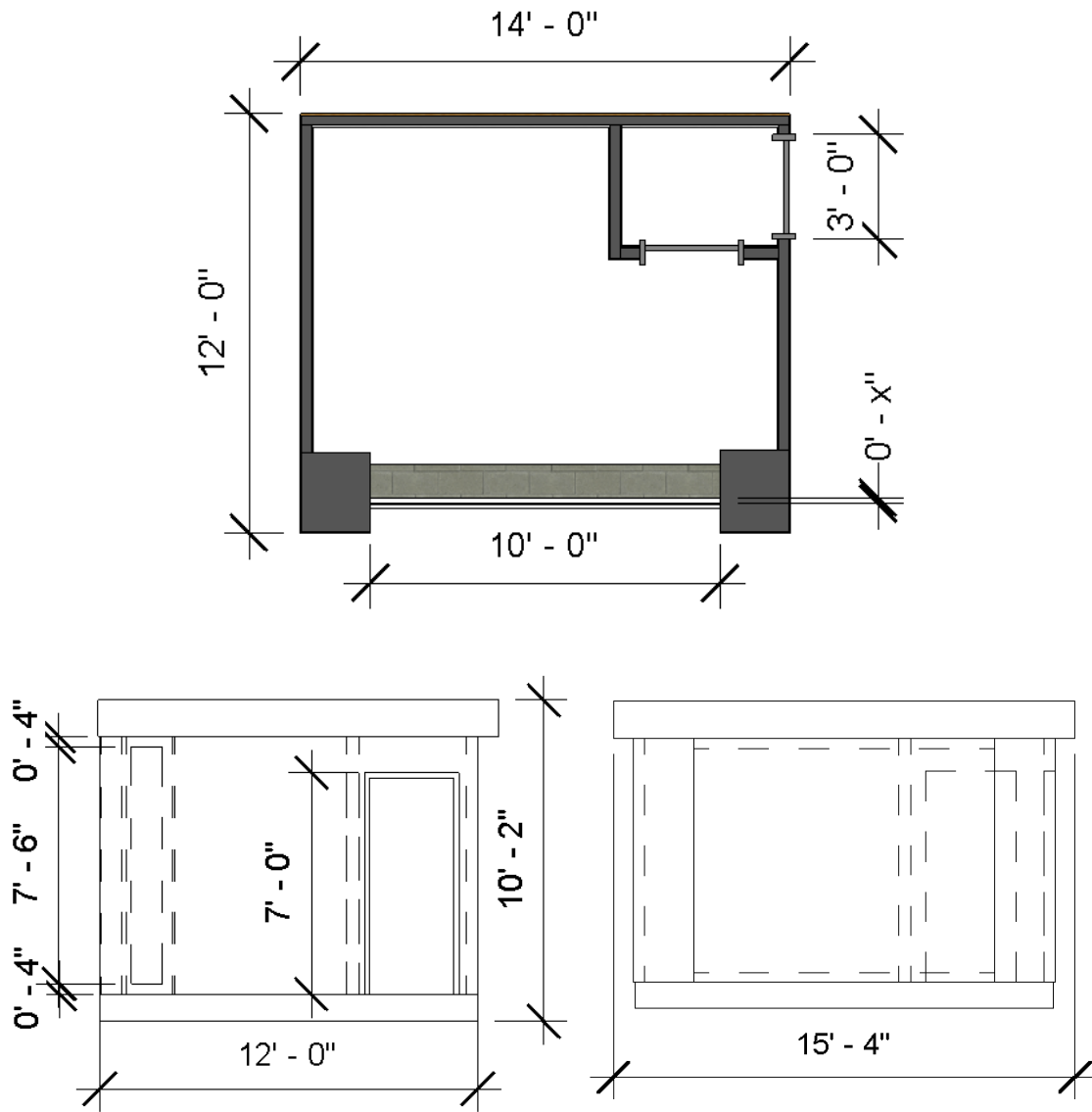
Figure 8. Vented created geometry plan view (top), east elevation (bottom left), and south wall elevation (bottom right) in Revit with dimensions.
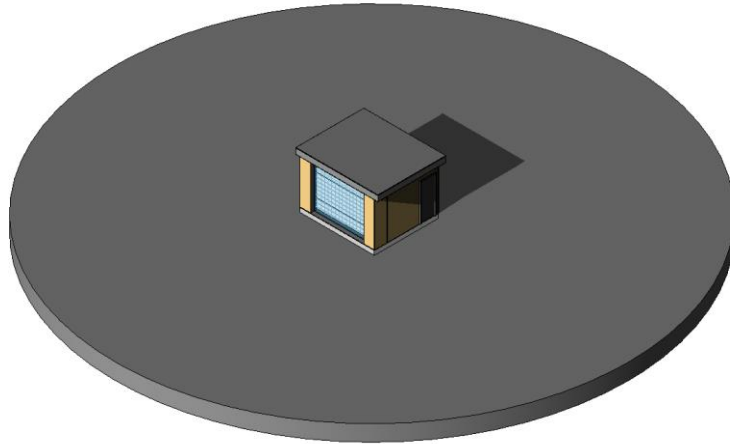
Figure 9. Three-dimensional view of vented model with ground volume.

An external volume of air around the structure was created to distance the source of radiation from the structure surface, allowing for shading to be accounted for. The external air volume must be large enough to allow both fully developed air velocity profiles and transfer of heat through convection. The width of the exterior air volume was extended the width of the previously defined ground volume, 100 feet. Autodesk suggested a height of at least three times the height of the test cell (*Solar Heating*, 2016). A height of 50 feet for both models was used. A domed environment volume, as seen in Figure 10, was chosen so that only one surface needed to be selected when defining environmental boundary conditions.
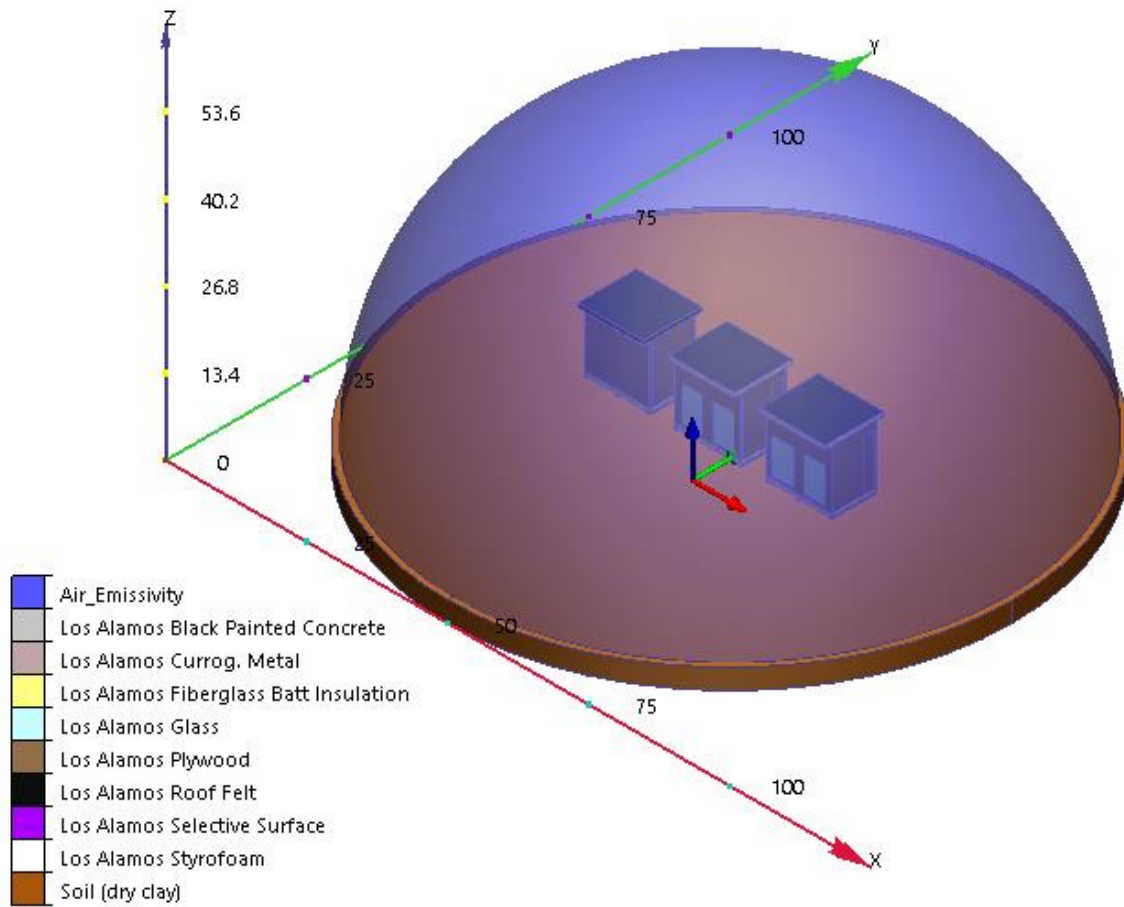
Figure 10. Domed air environment and ground volume surrounding unvented model in Autodesk CFD.

Defining Materials

Solid materials were defined by conductivity, density, specific heat, emissivity, transmissivity, and roughness. These properties, if not stated in the experimental study report, were estimated based on similar material properties from derived research (Ellis, 2003) or from the Autodesk material database. The properties of the glazing and mass wall require the most exactness. The properties of the mass wall determine how much heat is stored and how long it takes the energy to reach the interior. The transmissivity of the glazing determines

how much solar radiative energy reaches the air gap and mass wall surface. The properties of
all the construction materials are listed in Tables 2 and 3. The dry clay soil type in the
Autodesk material database was chosen for both models as this best represented the
predominantly arid soil type of the western United States. The soil properties are included in
both construction material tables.

κ	Thermal Conductivity (W/m-K)
ρ	Density (kg/m^3)
c_p	Specific Heat (J/kg-K)
ε	Thermal Emissivity
τ	Solar Transmissivity

Table 2

Material Properties for Unvented Study (LANL)

Material	κ	ρ	c_p	ε	τ
Black Painted Concrete	1.385	2189	510	0.9	
Corrugated Metal	45.3	7833	502	0.2	
Fiberglass Batt Insulation w/ studs	0.0459	84.8	963	0.9	
LANL Glazing (Thermopane)	0.9	2700	840		0.69
Gypsum Wall Board	0.17	800	840	0.8	
Plywood Sheathing	0.115	545	1213	0.9	
Asphalt/Ply Sheet Roofing	0.19	1121	1674	0.9	
Selective Surface	392.6	8906	370	0.07	
Styrofoam	0.0305	28.8	1213	0.8	
Soil (dry clay)	0.25	1600	890	0.92	

Table 3

Material Properties for Vented Study (EEG)

Material	κ	ρ	c_p	ε	τ
CMU Mass Wall (lightweight aggregate)	1.100	1432	879	0.85	
CMU Mass Wall (heavyweight aggregate)	1.100	2306	837	0.85	
Blown in Cellulose Insulation w/ studs	0.035	60	1944	.85	
Laminate Flooring	0.260	432.5	837	0.6	
Sunlite Premium II Kalwall Glazing	0.78	2700	840		0.88
Gypsum Wall Board	0.17	800	840	0.5	
Plywood Sheathing	0.115	545	1213	0.9	
Asphalt/Ply Sheet Roofing	0.19	1121	1674	0.9	
Wood Doors Hollow-Core	0.12	510	1380	0.8	
Soil (dry clay)	0.25	1600	890	0.92	

Two concrete masonry unit types, lightweight and heavyweight aggregate, were simulated for the vented study model. The heavyweight properties were modeled first and resulted in a larger thermal lag than was indicated in the actual measurements. Properties of a lighter density concrete were input to test the ability of the simulation tool to account for varying material properties in the calculation of conductive heat transfer through the mass wall. The properties of the heavyweight concrete were from the Autodesk database while the properties of the lightweight concrete were the reported values (Casperson & Hocevar, 1979).

Air was the only fluid material used in this study and was defined by density, viscosity, conductivity, specific heat, and emissivity. The Autodesk default air properties were used with an adjusted absolute pressure based on the elevation of the site. For the Los Alamos unvented study, the environment pressure was set to 23 in. Hg at an elevation of 7,080 feet. The vented Energy Engineering Group environment pressure was set to 29.65 in. Hg at an elevation of 7,530 feet. To allow for convective heat transfer the air of the interior

30

and the exterior were set to variable. A variable material changes property with a change in environment. An equation of state is used to correlate the density of air to changing environment temperature and pressure. A decrease in air density with increasing temperature is what drives the buoyancy effect that creates the convective currents within the air gap of a Trombe wall.

The emissivity property of the air could also be adjusted over time or in relation to temperature. The emissivity property in Autodesk CFD relates directly to the reflectivity of the solid surface or fluid (*Solar Heating*, 2016). The sum of reflectivity and emissivity of the surrounding air volume total to one. A high emissivity value for the exterior air volume means little to no solar radiation is reflected before reaching the test cell model surfaces. A lower emissivity could represent a high reflectivity due to intermittent cloud cover. The emissivity of a clouded day, see 2/14 and 2/18 of Figure 11, was based on the percentage difference to solar insolation measured on the proceeding clear sky day. The unvented simulation with varying emissivity values was not able to run successfully without diverging. Only clear sky days were reported for the vented study. Only two days of the eight days reported for the unvented study indicated clouded conditions. Therefore, a constant emissivity rate of 0.8 was used for the exterior air volume of both studies.
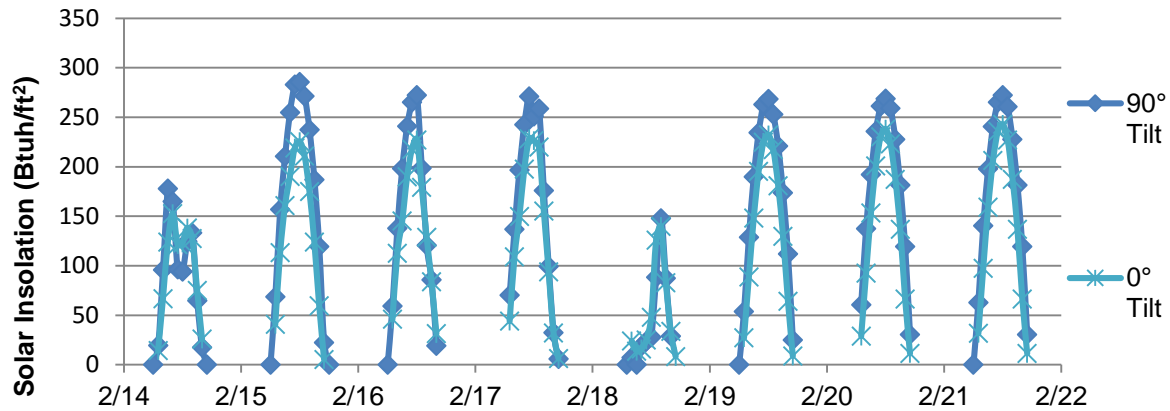
Figure 11. Measured solar insolation from 2/14 to 2/22/1982 at Los Alamos National Labs. Measurements were taken with a pyranometer at 90° and 0° tilt.

Defining Boundary Conditions and Initial Conditions

Boundary conditions were created based on local weather to simulate both solar radiation and ambient air temperature. Transient (time-varying) analysis was used to take into effect the changing exterior climate on the interior air volumes. Conditions such as film coefficients, total heat generation, and flow rate were considered when accounting for wind flow, auxiliary heat, and fans respectively. Due to solver errors and divergence some of these considered conditions, such as auxiliary heat and fans, were not able to be included in the final model simulations. Two different methods of initializing the conditions of the test cell materials were used depending on available data from the experimental studies.

Location and weather.

The first study used for validation is located at Los Alamos National Labs in Los Alamos, New Mexico, at 35° 48' N Latitude and 106° 18'W longitude, at an altitude of 7080ft. The air pressure is estimated to be 23 in. Hg at this altitude. These test cells were monitored hourly, mainly in winters, between 1979 and 1982. Accessibility to both

monitored cell data and weather data within these three years narrows the time frame used in this study to between February 14 and February 22, 1982.

The vented study was conducted in Idaho Springs, Colorado at 39° 44'° N, 105° 30'° W. Atmospheric pressure is 29.65 in. Hg. Each configuration was tested 3 times for 5-7 consecutive hours on clear days in January and February of 1979. The measured variables include temperature and air velocity at the glazing surface, mass wall surface, within the air gap, and within the inlet and outlet vents.
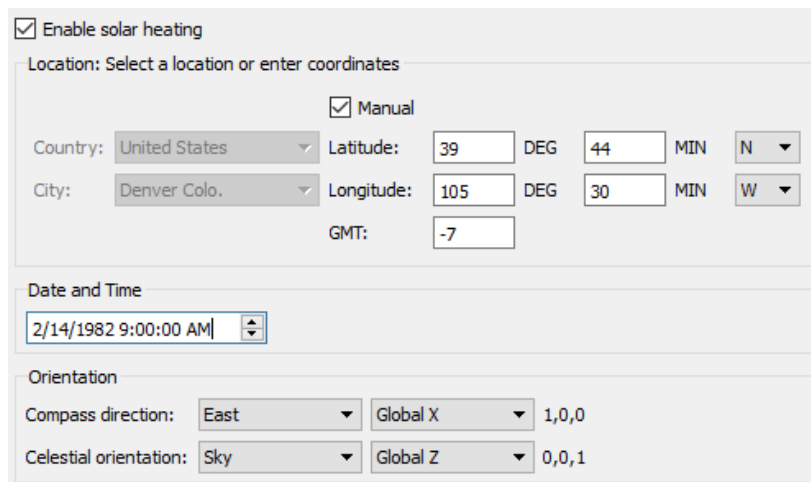
Wind and film coefficients.

An estimation of a convective film coefficient for all exterior boundaries was used to incorporate ambient wind speed from the weather data into the model. This boundary condition enables solid elements to transfer heat to the exterior air volume if no velocity boundary conditions are set. Tests were run prior to setting an exterior air volume or film coefficient boundary which led to a constant increase in the temperature of the model interior and structure.

To incorporate the entire wind flow field as a function of time and direction would be too labor intensive for design modeling purposes. The approach used in this model was an average film coefficient for all exterior surfaces. Both test cells were low-rise and in low wind speed regions (0 mph to 5 mph). In low wind speed regions, the film coefficient is driven mainly by natural convection and can be calculated from temperature difference between the exterior surface and the ambient temperature (Yazdanian & Klems, 1994). Temperature differences between 20 and 40°F in low wind speed regions for both windward and leeward surfaces result in film coefficients between 3 and 5 W/m^{2}K. A film coefficient

33

of 4 W/m^{2}K with a reference to transient ambient temperature was used as a boundary condition on all exterior surfaces.

Solar heating analysis.

Solar radiation through the glazing of the Trombe wall drives both the buoyant air flow in the air gap and provides energy to be stored within the absorptive thermal mass. Solar heating in Autodesk CFD can simulate the effect of solar heat radiating onto structures using the Radiation solver (Solar Heating, 2016). In the Physics tab of the Solver the date, time, and orientation of the structure can be input into the solar heating dialog (as seen in Figure 12). In the heat transfer dialog, the direction of gravity was defined as (0,0, -1) and east was defined in the direction of the positive y-axis.

Figure 12: Solar heating dialog in Autodesk CFD 2016. Location and time of vented study are input manually.

From these inputs, the sun position is calculated and will change with respect to time during a transient analysis. The default solar heat flux is defined in the flag manager as 910 W/m^2. This value was manipulated for each simulation based on the maximum insolation value measured within the corresponding test. The maximum solar heat flux measured for a

vertical surface during the eight days of unvented data was 285.4 Btuh/ft^2 (1603.5 W/m^2).

The maximum values of solar insolation on a vertical surface for the vented study ranged

between 268 and 304 Btuh/ft^2.

During the simulation, the solar heat flux could be visualized and verified to actual

measured values. Figure 13 shows the result quantities of solar heat flux on the surface mesh

elements at 4:00pm. As expected, during the evening the east wall is mostly shaded while the

south and west wall are receiving a majority of the solar radiation. The solar heat flux value

on the exterior surface of the south facing glazing of the model was between 320 and 360

W/m^2. The corresponding measured value at the same time was 60 Btuh/ft^2 (340.7 W/m^2)

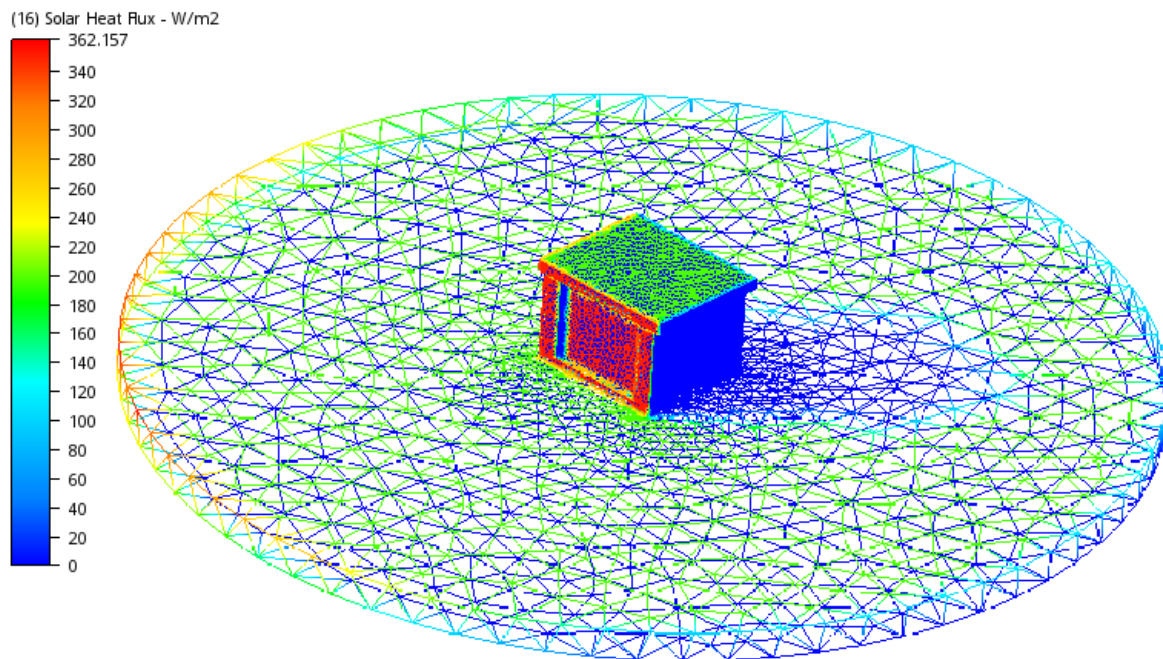which matches well with the model values.

Figure 13: Solar heat flux displayed on the mesh of vented model.

Exterior temperature.

The measured ambient exterior temperature was input as a .csv file into the solar heating study temperature reference dialog. The condition is set to transient and the piecewise linear function form was filled in with an imported .csv file that had temperature values in Fahrenheit change every 3600 seconds for the unvented study and 900 seconds for the vented study. Figure 14 shows the dialog for inputting transient temperatures as well as a plot for two days of hourly temperatures.
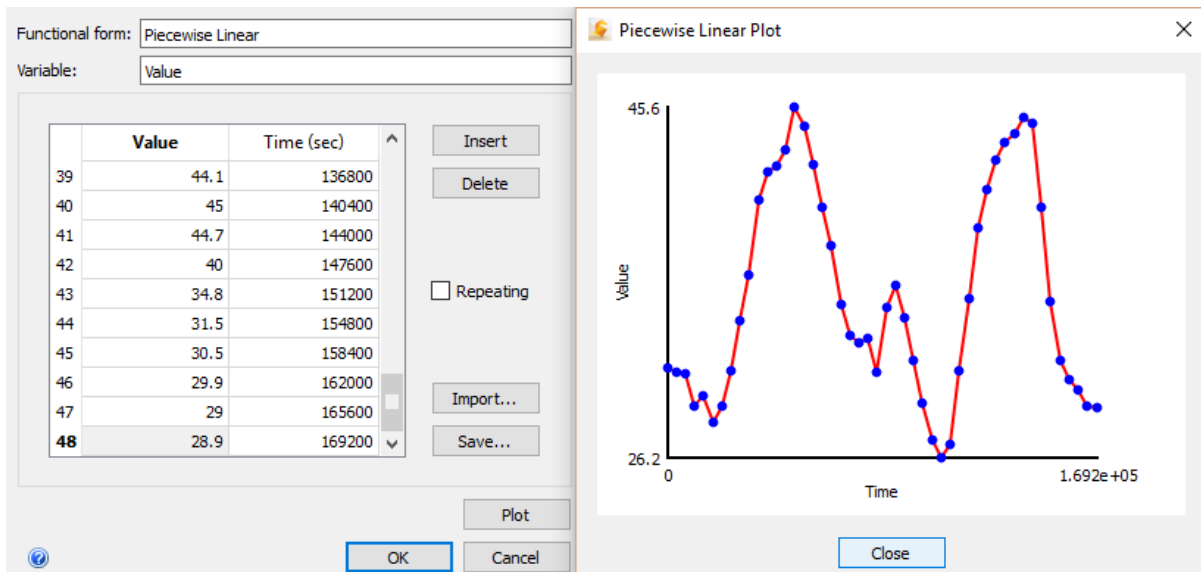
Figure 14: Transient piecewise linear function of temperature over two days.

Initial conditions.

The storage effect of the thermal mass is an important consideration when simulating passive solar buildings. The mass wall, depending on thickness and material properties, stores energy from solar radiation and warmer surrounding temperatures then emits this energy at night when the surrounding space is cooler. The energy stored in a mass wall at any time is dependent on how much energy was supplied and removed from multiple consecutive

days beforehand. The internally stored energy must be recreated in a simulation. This can be done by conditioning the model's solid geometry with multiple days of radiation and night temperatures. Or, if the temperature gradient of the mass wall interior is known, defining these conditions and conditioning the surrounding air flow in a steady-state analysis.

Two strategies were used to create the starting thermal condition of the mass wall and interior air space. These strategies were employed based on available data. For the unvented study, there were multiple consecutive days of data which could be used to condition the materials.

For the vented study, the initial conditions of the thermal energy stored within the mass wall were defined by the first hour of sensor data from the interior of the mass wall. The mass wall was split into 3 vertical zones and 4 horizontal zones. The temperature of these zones was determined by the average of the four surrounding thermocouples at 15-minute increments. The thermocouples were installed at 30 and 79 inches above the bottom of the mass wall at depths of 0, 1, 3, and 6 inches from the air gap surface of the mass wall. The zones of the vented wall can be seen in Figure 15. The zone temperatures at the first time step of each test were input into representative split volume zones of the model mass wall. Table 4 shows the initial mass zone and air temperature input for each vented model configuration. Initial conditions of the air volumes were set based on the measured values of the first time period in each study.

Table 4

Initial Conditions of Vented Model Mass Wall and Interior Air Temperature for Vented

| Model Test	Initial Air Temp	11	12	13	14	21	22	23	24	31	32	33	34
2inch_1	72.35	108.7	82.9	62.7	59.1	115.2	86.3	61.5	57	108.8	82.3	59.8	55.4
2inch_2	62	78.4	67.8	66	66.4	77.3	65.1	63.8	64.4	74.3	63.5	61.4	62.1
4inch_1	75.6	91.9	84.6	83.8	83	90.8	82.7	81.6	80.8	86.6	79.8	78.5	77.9
4inch_2	79	93.7	86.7	86.7	86.1	92.5	84.9	84.7	84.3	89	82.5	81.9	81.8
6inch_1	68.95	82.5	75.6	74.8	73.7	80	73.3	72.9	72.3	77.6	71.2	71	70.9
6inch_2	66.3	82.7	70.7	63.7	61.9	91.3	74	63.7	61.1	88.6	72.3	62.4	60.1
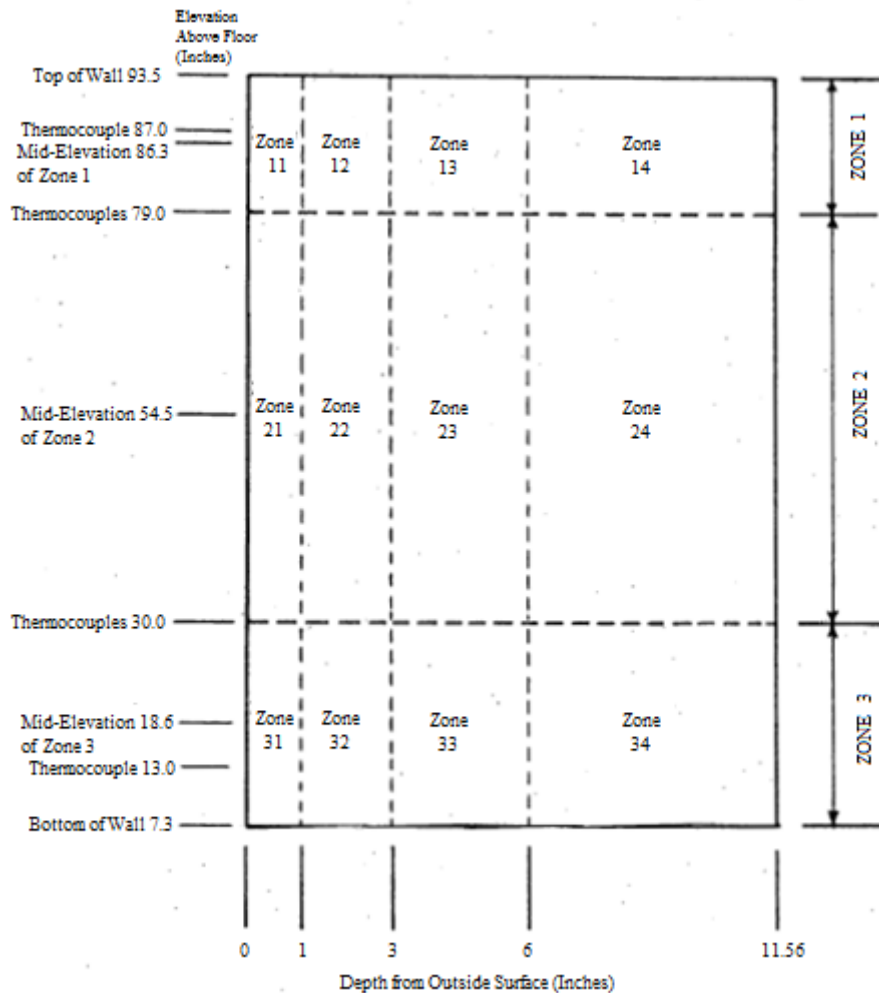
Figure 15. Monitored zones for thermal energy storage for EEG vented study.

Auxiliary heating and ventilation.

The Los Alamos study used average power measurements from light bulbs to gauge passive heating performance. The interior temperature of cells 1, 2, and 11 was maintained at 65°F by a 500W light bulb. The light bulb would be off while the sensor in the center of the room read temperatures above 65°F and would turn on when the measurement read below. The power rating of the light bulbs was added whenever a scan indicated that the cell was receiving auxiliary heat. The accumulated sum was divided by the number of scans to obtain the average hourly power used by the light bulbs in watts. Cell 12 had no auxiliary heating. The auxiliary heat in cells 1, 2, and 11 were accounted for in the model using the total heat generation boundary condition. This condition was applied to a volume of comparable size to a light bulb within each cell. The hourly averaged power was input into a piecewise linear table for each cell. The auxiliary heat for cells 1 and 2 are shown in Figure 16. The EEG study had no source of auxiliary heat. When total heat generation was included as a boundary condition the interior temperature would increase rapidly before the simulation diverged and terminated. This may indicate an improper application of the total heat generation boundary condition or an improper representation of the light bulb heat source. There were light emitting diode (LED) materials in the Autodesk database, but these required PCB components.
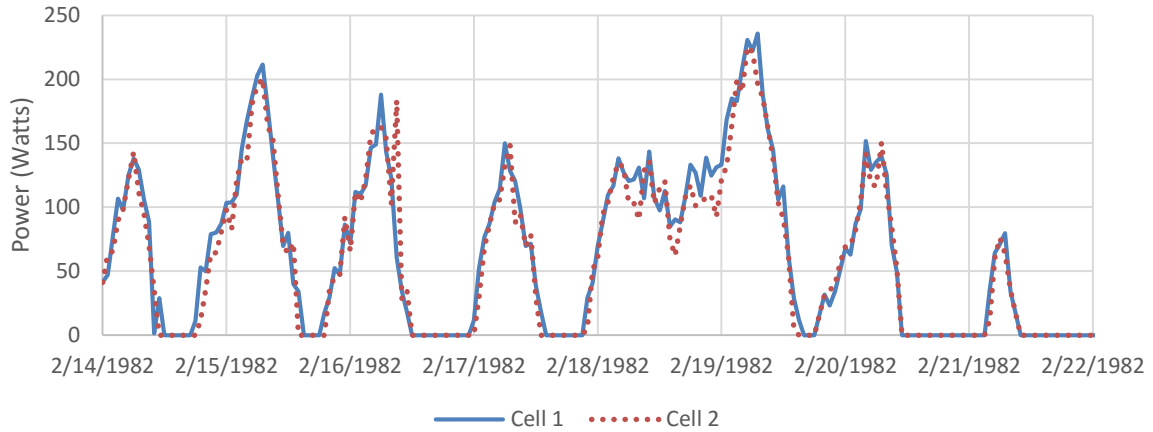
Figure 16. Auxiliary Heat of Los Alamos Test Cells 1, 2, 11, & 13.

The Los Alamos study also used mechanical centrifugal fans with a constant flow rate of 1125 ft^3/h (0.00875 m^3/s) in order to pressurize the geometry and reduce unknown infiltration (Ellis, 2003). This air change rate was a nominal value standardized to atmospheric pressure at the test cell elevation. Only cells 1 and 2 of the modeled cells had fans. Fans were represented in the model using a geometry of similar size and a constant flow rate boundary condition of 0.00875 m^3/s. The inclusion of the flow rate boundary condition as a representation of the mechanical fan similarly resulted in the simulation reaching divergence before completing the allotted time. No fans were used in the vented study and the infiltration was not included in the referenced report, attributing further to uncertainty in the model results.

Creating the Mesh and Solving Parameters

The mesh and the solving parameters chosen have a large impact on how quickly and how well the simulation can run, especially in a transient analysis. The processing power of

the simulation computer used also affects the computational time. A computer with a 2.3 GHz processor and 4GB of RAM was used for all simulations.

Volume based mesh auto sizing was used with finer mesh sizing on volumes where sensors were located. Once the mesh was automatically sized the glazing and mass wall volumes were selected and refined. The automatic mesh sizing tool in Autodesk CFD breaks the geometry into tetrahedral volumes. The flow and heat transfer partial derivative equations are solved across nodes of the tetrahedral mesh within each time step. Once the mesh was automated and regionally refined it was visually verified that at least two nodes were across all material thicknesses to allow heat to transfer more accurately. Both the surface and gap refinement tool proved useful when defining the mesh. The difference between a coarse mesh and fine mesh definition of the vented test cell is shown in Figure 17. The model with the coarse mesh, composed of 51 thousand solid volumes, took approximately two hours to complete an eight-hour transient analysis using a time step size of 60 seconds. The fine mesh definition, composed of 1.35 million solid volumes, took approximately 16 hours. A combination of a coarse and fine mesh was used.
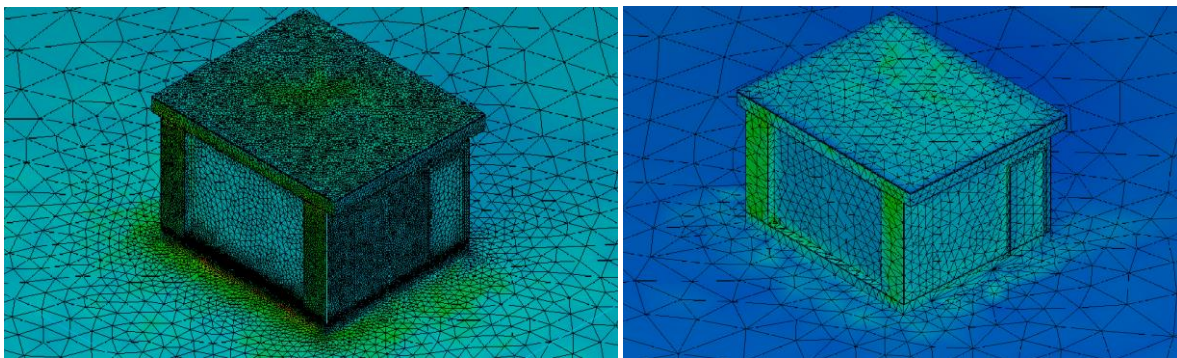

Figure 17. Coarse mesh (right) and fine mesh (left) of the vented model.

There are multiple turbulence models available in Autodesk CFD. Studies have used k-epsilon and renormalized groups to numerically solve heat transfer in the air gap of Trombe walls (Zamora & Kaiser, 2009). In most indoor environmental analyses, a standard k-epsilon model can provide satisfactory results (Chen & Srebric, 2002). For this study k-epsilon was chosen as the turbulence model. Both low Re and RNG were attempted but they either took more computational time than necessary or could not reliably complete the full time frame of the simulation without diverging. Apart from the turbulence model an advection scheme must be chosen. The advection scheme determines the numerical method of propagating results of surface elements through the solution mesh. The advection scheme suggested for transient heat transfer and for pressure driven flow analyses was the Petrov-Galerkin numerical method (Troubleshooting - Advection Schemes, 2014). Advection scheme 2 was used at first but often led to divergence in the CFD system of equations. Advection scheme 5 proved to be a more stable method for both models.

Monitor Points and Data Analysis

In order to validate the CFD simulations, the same variables must be measured in the simulation as were measured in the experimental test cells. This requires that monitor points are placed in the model in the same location as the sensors are reported to be located in the actual test cells. For the unvented study this is mid-height and center on the south and north wall and in the middle of the interior air space 6 feet high for each cell. A cross section of the center plane, as well as the south wall elevation, show the approximate location of the sensors (as seen in Figure 18). The measured values from the sensor points over eight consecutive days are displayed in Figures 19 and 20. Type K thermocouples were used which have a graded accuracy of +/- 0.75% or +/-2.2°C (McFarland, 1982; Thermocouples, n.d.).
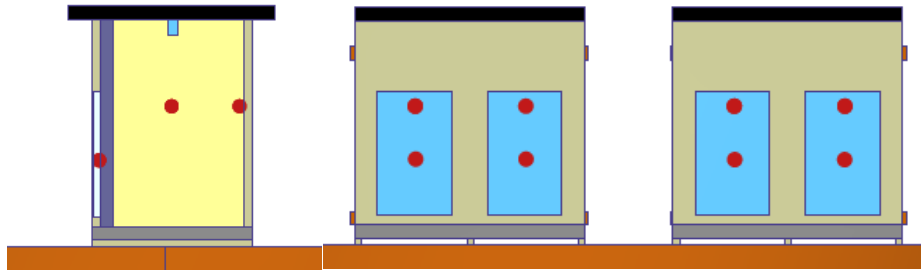
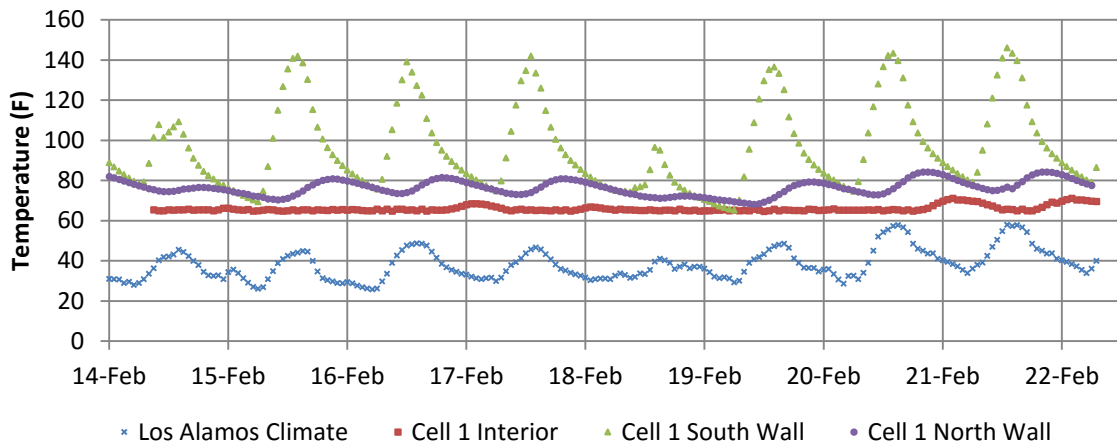*Figure 18.* Location of Los Alamos test cell monitor points in section view (left) and south elevation (right).

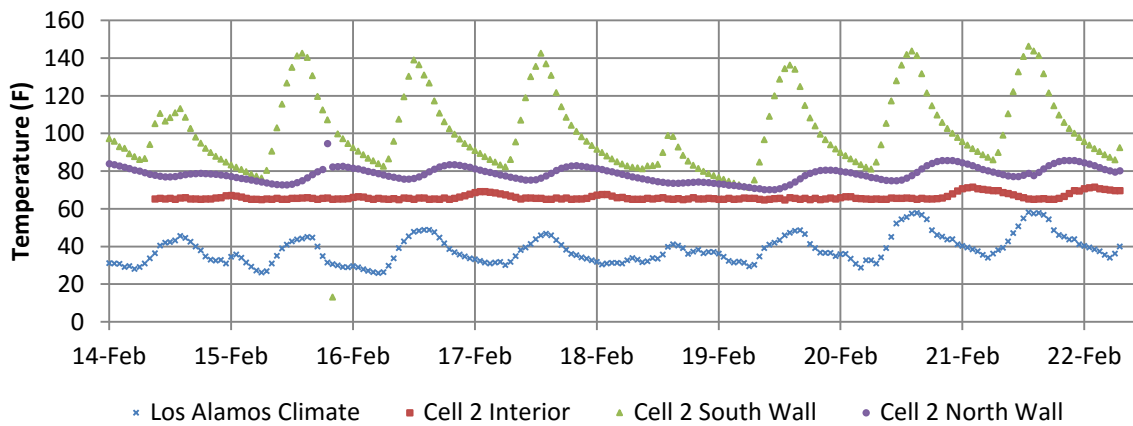*Figure 19.* Los Alamos test cell 1 interior and exterior temperatures.

Figure 20. Los Alamos test cell 2 interior and exterior temperatures.

For the vented study there were both thermocouples and velocity probes set throughout the air gap and mass wall. The main sensors of interest are the temperature sensors centered in the duct gauging the temperature of the air entering and leaving the air gap. There were velocity probes set at 24 inches from the floor of the centerline. The probes were set on the inside surface of the glazing and every 0.5 inches till the surface of the mass wall. The readings of temperature sensors at 13, 30, 79, and 87 inches in height on the centerline and along the inside surface of the glazing and air gap surface of the mass wall were also compared. The approximate locations of the sensors in the model, including those discussed earlier within in the mass wall, can be seen in Figure 21. The thermocouples were calibrated to +/- 0.75 °F while the velocity probes were accurate to +/-5.3% for velocities exceeding 0.3 ft/sec (McFarland, 1982).
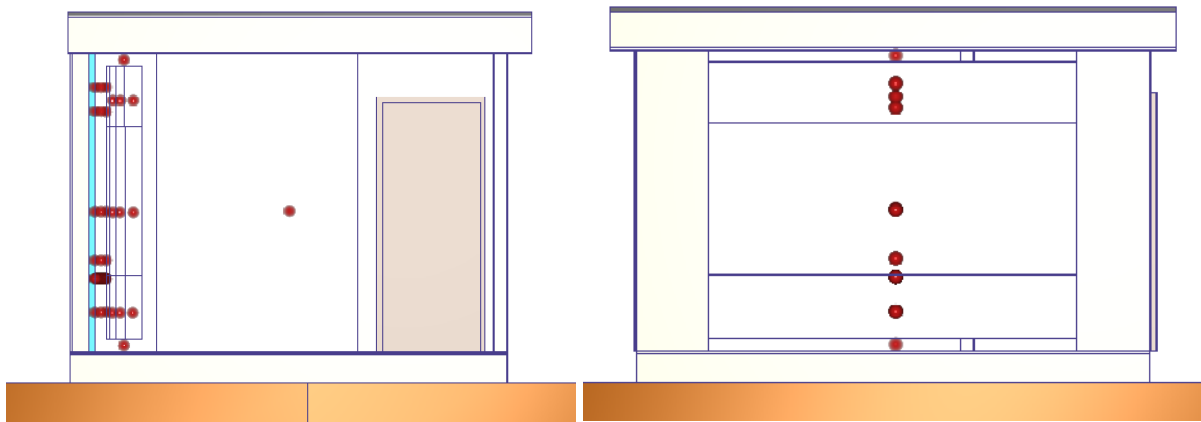

Figure 21. Location of 4-inch gap vented model monitor points in section view (left) and south elevation (right).

Chapter Four: Results and Discussion

Visualizations of Air Flow Patterns

In Autodesk CFD, there are many options when visualizing the results of a simulation. The plane feature was used to view the results within the same plane that the actual sensors were installed, centered horizontally. Further visualization, mainly using the global results tool shown in Figure 22, was performed to ensure that believable values existed throughout the model. The visualized results of multiple time steps can be viewed if a save interval was defined in the simulation parameters. This feature was used when checking that solar heat flux values were tracking appropriately over time. Results of the most recent time step can also be seen during the simulation. If the temperature and air velocity of the interior space exceeded a believable range during the simulation it was expected that there was an error and the simulation was about to diverge. Visualization was useful in monitoring how boundary conditions behaved; it was most useful when monitoring how the interior air fluid reacted to these boundary conditions.
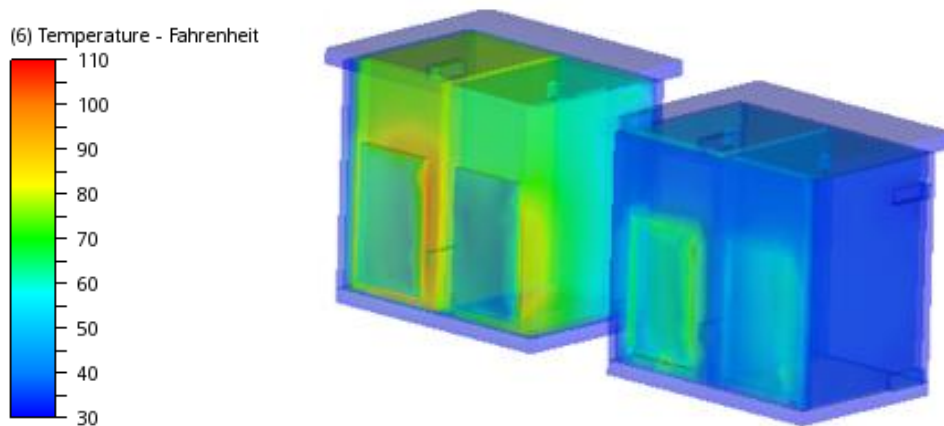

Figure 22. 3D global visualization of temperature gradient in Los Alamos model.

The plane visualizations of the models show an expected air flow as a result of the

solar heat gain of the Trombe wall. In the vented system of the EEG study, a negative

pressure is created within the air gap between the glazing and mass wall. This negative

pressure brings air from the room into the air gap. The air in the air gap is then heated

causing it to elevate and redistribute into the room through the top duct. The expected

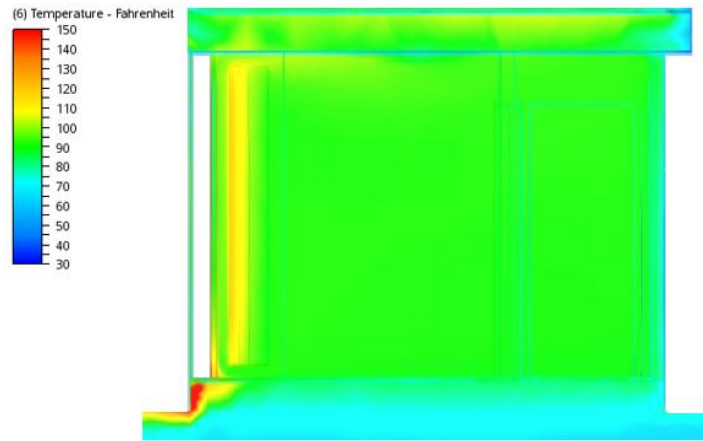buoyant air flow is seen in Figure 24.

Figure 23. EEG vented model temperature distribution along the center horizontal plane, 4inch air gap at 4:30pm Feb 14, 1979.
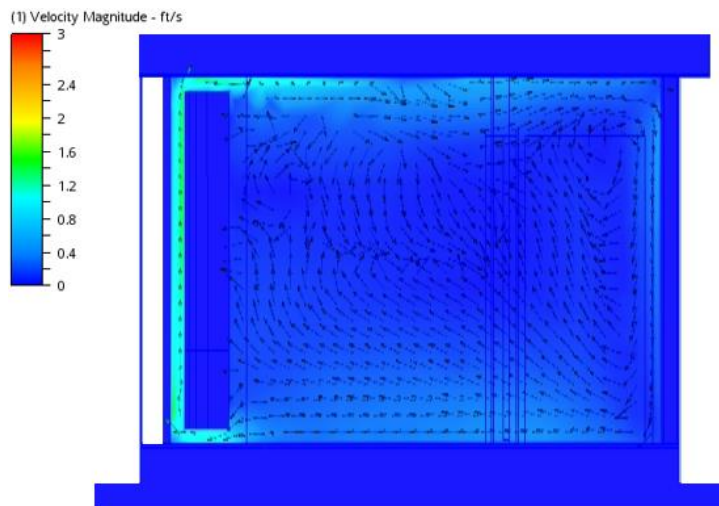

Figure 24. EEG vented model velocity magnitude plane and vector profile along the center horizontal plane, 4inch from 4:30pm Feb 14, 1979.

The unvented Trombe wall configuration of the Los Alamos study likewise causes a buoyant air flow on either side of the heated mass wall, sometimes competing with air circulating in the room. From the visualization of cells 1 and 2, it seems as though the temperature of the mass wall and room increase the circulation of the air rises and becomes more concentrated on the mass wall. While there were not air velocity sensors in the unvented study it was assumed that the values fell within a believable magnitude range determined by ASHRAE 55 comfort standard. Temperature ranges were slightly higher than expected for winter conditions though still within believable ranges.
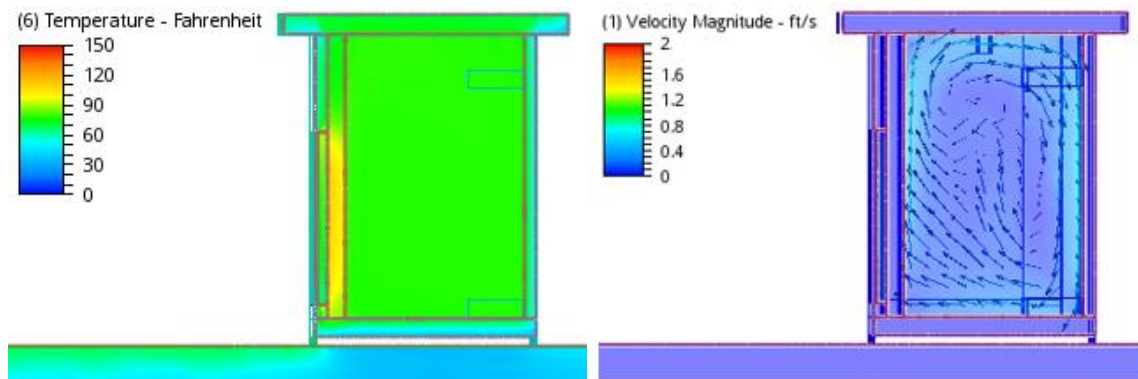

Figure 25. Los Alamos Labs test cells 1(left), 2 (right). An example of temperature distribution and air flow. Results correspond to climate data input from 2/15/82 at 2:00PM.

Viewing the results through two-dimensional slice or planes allows the user to view the temperature and air velocity field within regions normally occupied by people. ASHRAE 55 defines the occupied zone as within 6 feet above the floor, more than 3.3 feet from exterior walls, and 1 foot from interior walls (ASHRAE, 2010). The suggested temperature difference from approximately ankle level to head height is 5.4° F. An ideal air velocity in winter months would be below 0.5 ft/second or below 0.8 ft/second in summer months. While these ranges of acceptable thermal comfort conditions vary depending on other

47

conditions such as exterior climate, clothing, and activity level they give a good starting point when gauging the performance and plausibility of the simulated models. The final simulations for both the unvented and vented models showed believable temperature ranges and expected buoyancy driven air flow direction and magnitude.

Monitor Points Results

While visualization of results can be important in design optimization and problem area identification it is the purpose of this study to look at the accuracy of the model in relation to point measurements of temperature and air velocity. The results of the unvented study showed a similar sinusoidal diurnal pattern did exist the amplitudes did not compare. The vented study showed much better agreement to actual results though there was still a consistently lower temperature in the model data around midday.

The Los Alamos study was chosen to see whether the model could recreate a similar sinusoidal interior temperature pattern due to multiple diurnal cycles. The simulated results for cell 1 and 2 can be seen in Figures 26 and 27, respectively. These simulations were run with a time step of 3600 and 5 iterations within each time step. The conditioning method of the unvented study was able to stabilize the results to a diurnal pattern similar to actual within the first two or three days. However, comparing the air gap temperatures resulted in a maximum temperature difference of 55° at peak solar insolation. The interior temperatures are consistently within 10° of one another after the initial two or three days of conditioning. The day with the least amount of error between actual and model was 2/18 which reported solar insolation values much lower than surrounding clear sky days. Two possibilities for this error are that the radiation condition was not accurately defined or the radiative heat transfer

through the Trombe wall materials is not appropriately accounted. The latter could be due to variance between reported material properties and actual. If the transmissivity of the glazing was lower than the reported value, it would allow more solar radiation to reach the air gap and mass wall, increasing the temperatures. There is also the possibility of inaccurately measured data. The temperature sensors were shielded but may have recorded much higher temperatures if exposed to direct solar radiation through the glazing. It should also be considered that these simulations did not include the reported auxiliary heat and fan which would affect the overall accuracy.
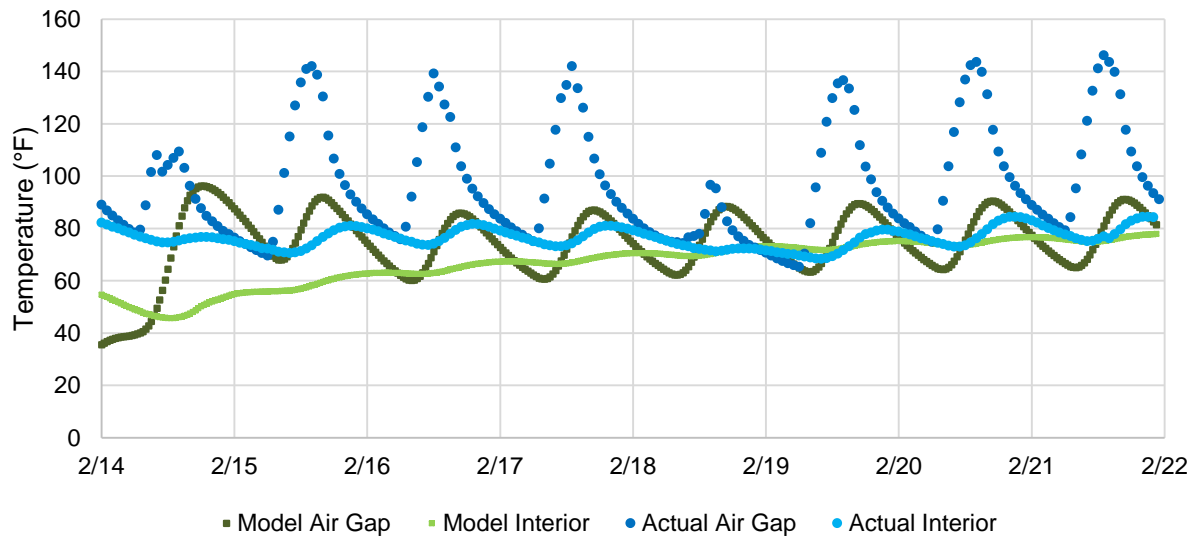

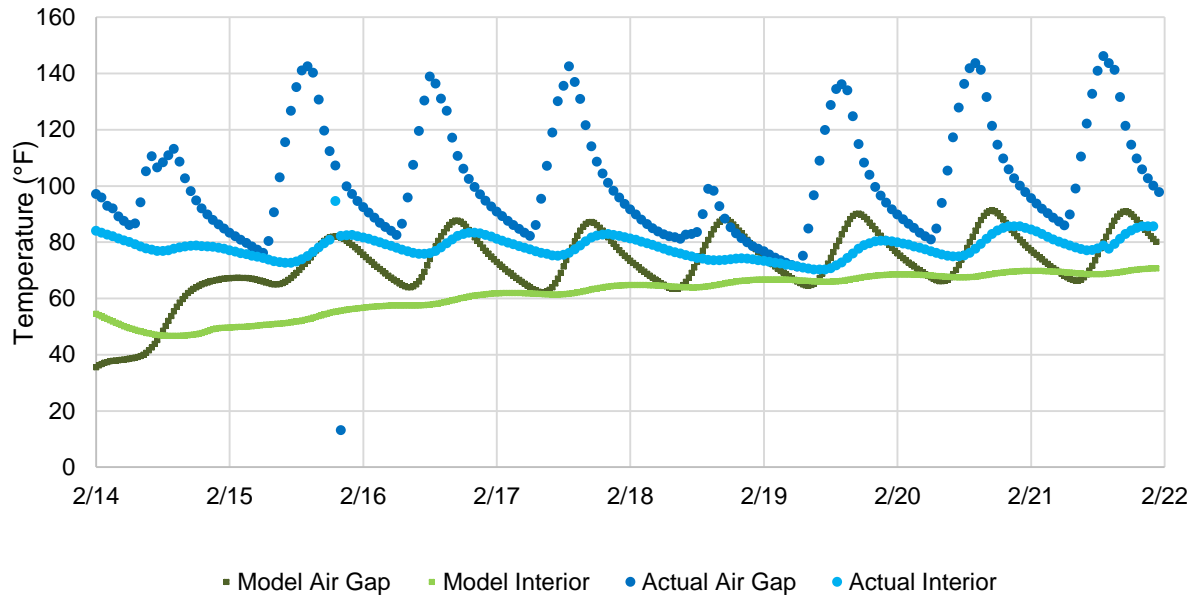*Figure 26.* Los Alamos cell 1 model results compared to actual.

Figure 27. Los Alamos cell 2 model results compared to actual.

The vented study had measured data for the interior of the mass wall. This data was used to both condition the initial internal temperatures of the mass wall and to test the ability of the CFD tool to account for conductive heat transfer. The low conductivity and high specific heat of the mass wall material slow the transfer of heat to the interior. The energy obtained from midday, a period of peak solar insolation, is offset and slowly distributed to the interior space during periods of no solar heat gain. Figures 28, 29 and 30 show the comparison between measured and simulated internal wall temperatures at 13, 46, and 79 inches in elevation and centered horizontally on the mass wall. The results of the vented model with a heavyweight concrete defined are shown in Figures 28 to 30 and the lightweight concrete model results are shown in Figure 31 to 33. The vented study only reported daytime values. Realistic night temperatures were input for the simulation of the

heavyweight concrete in order to see whether the model mass wall temperatures were
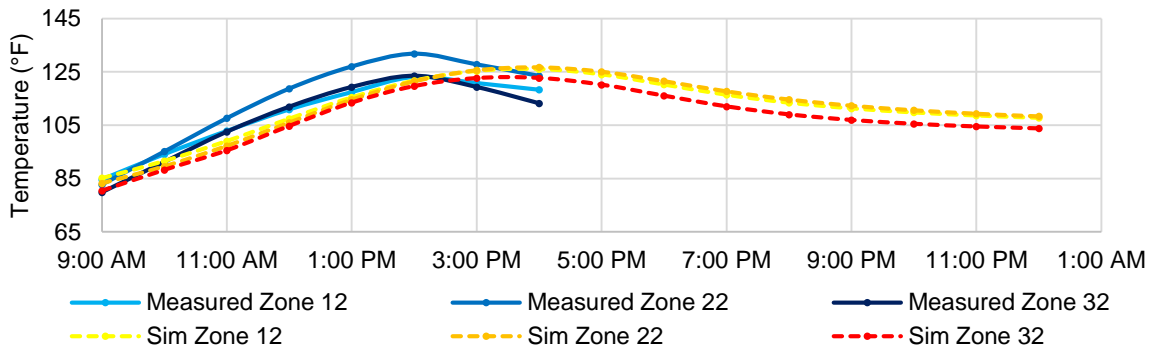plausibly maintained without a source of solar radiation.

Figure 28. Internal heavyweight mass wall temperatures of the first 1 to 3 inches away from the glazing. Simulated 4inch vented model compared to measured data.
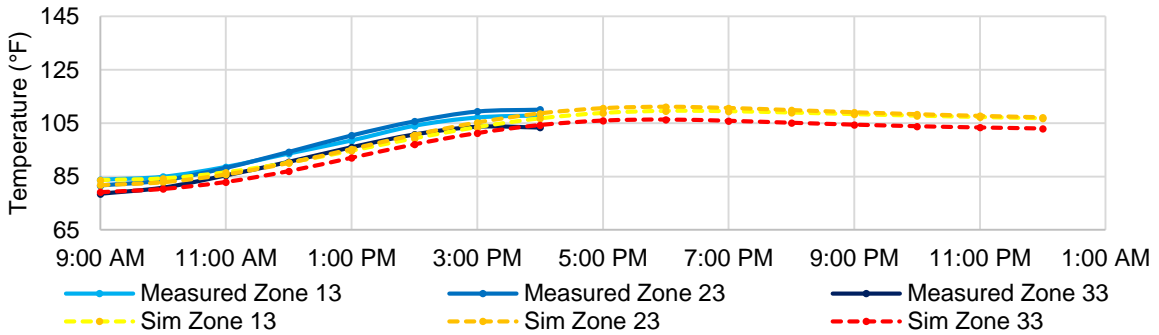

Figure 29. Internal heavyweight mass wall temperatures of first 3 to 6 inches away from the glazing. Simulated 4inch vented model compared to measured data.
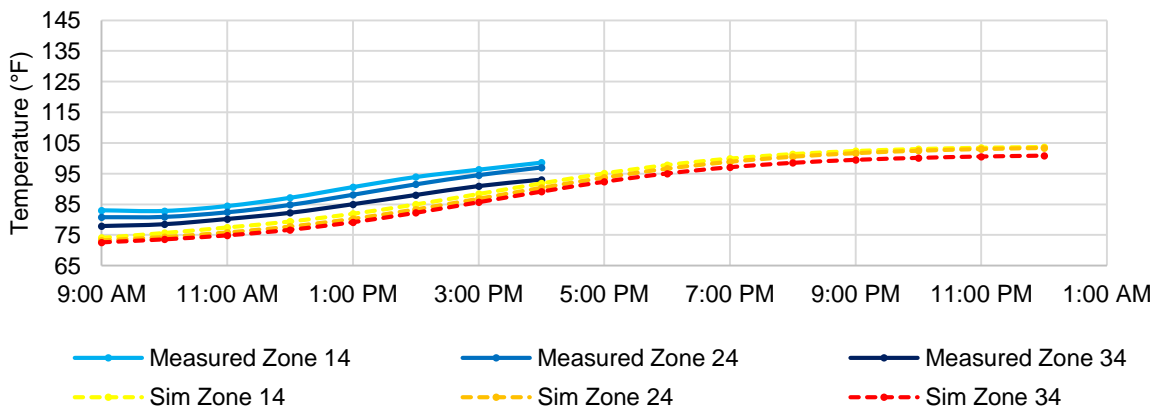

Figure 30. Internal heavyweight mass wall temperatures of 6 to 12 inches away from the glazing. Simulated 4inch vented model compared to measured data.

The peak temperatures of the layer nearest to the glazing, 1 to 3 inches, was approximately two hours earlier in the measured data than in the simulated data. The peak temperature of the 6 to 12 inch zone was much lower and much later in the day. The ability of the interior layer of the mass wall to maintain temperature agreed well with the expected thermal lag characteristics of the Trombe wall. A higher density or lower specific heat would slow the heat transfer through the masonry and result in a later peak temperature in the model. The model with the lightweight properties showed a closer depiction of the actual internal mass heat transfer. The center vertical zones showed the highest temperatures in both models similar to actual. The simulated peak temperatures of the 1 to 3 inch zone were lower in both the heavyweight and lightweight model. Consistently lower temperatures further suggest a discrepancy between input radiation conditions and actual solar radiation.
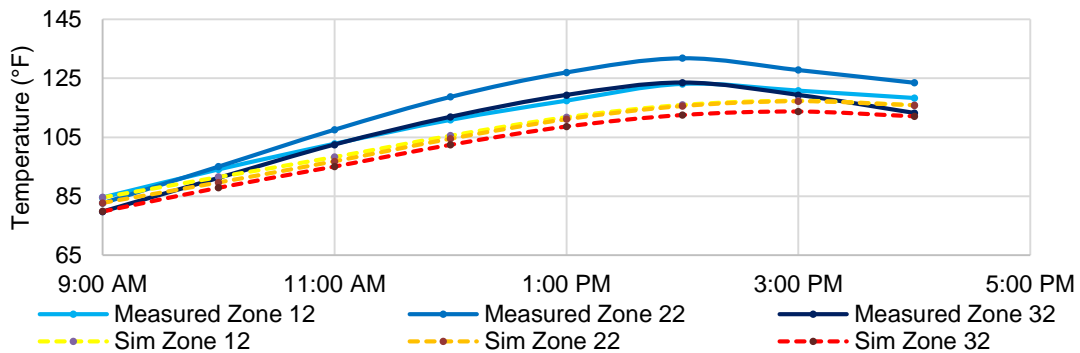

Figure 31. Internal lightweight mass wall temperatures 1 to 3 inches away from the glazing.
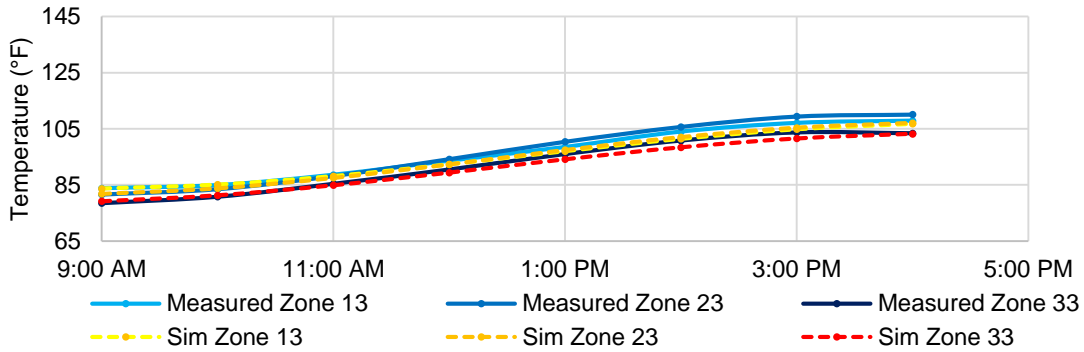
Figure 32. Internal lightweight mass wall temperatures 3 to 6 inches away from the glazing.
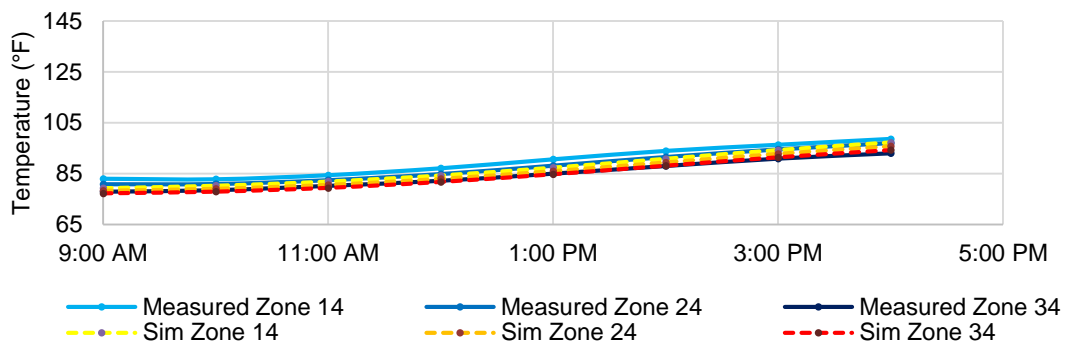
Figure 33. Internal lightweight mass wall temperatures 6 to 12 inches away from the glazing.

The direct comparison of temperatures within the inlet and outlet ducts of the vented wall study show a common pattern of lower predicted temperatures midday. Figures 34, 35, and 36 show the vented 2, 4, and 6 inch gap model results compared to actual results. The results of the following simulations were run with time steps of 60 seconds. The model takes a few iterations to level out the difference in temperatures between the ducts as the air flow and convective heat transfer is initialized. This initial temperature was set based on the temperature of the interior space at the first recorded time. With a 60-second time step, it would appear the temperatures of the inlet and outlet duct are able to stabilize within the first hour of the simulation.

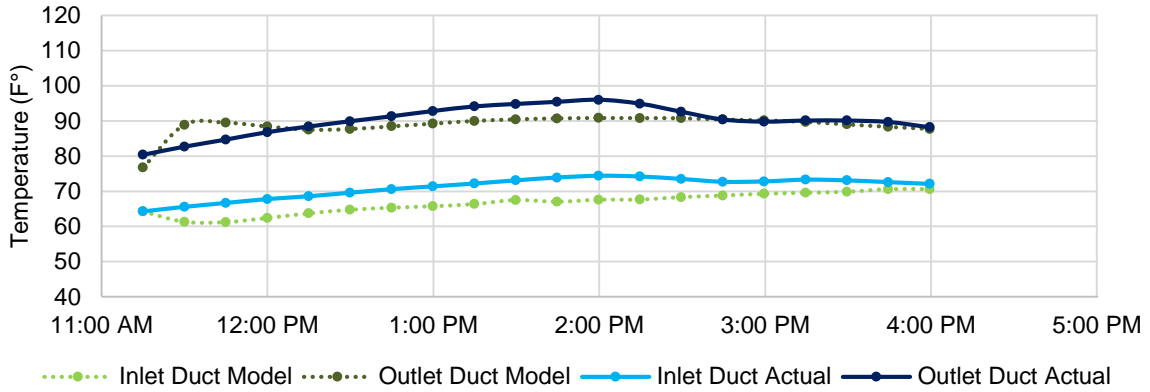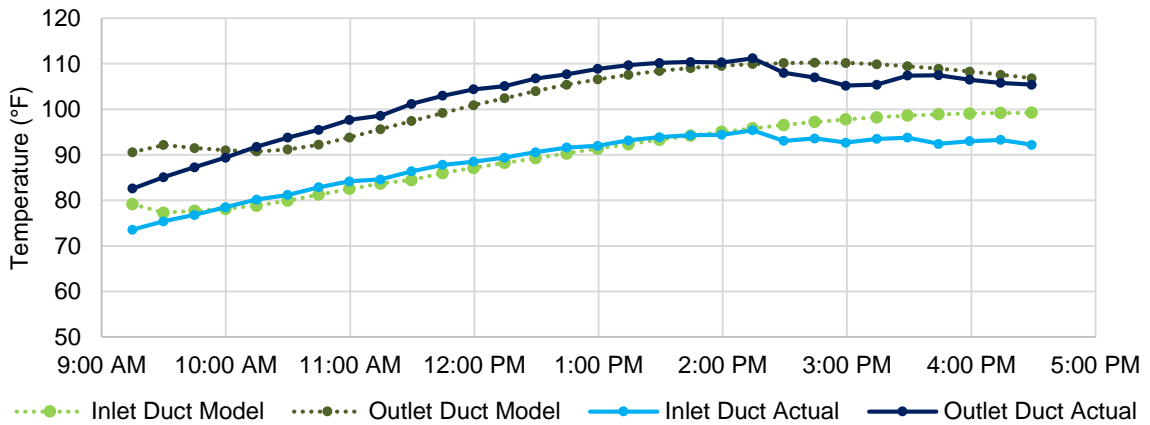*Figure 34.* Actual inlet and outlet duct temperature compared to 2inch gap model results.

Figure 35. Actual inlet and outlet duct temperature compared to 4inch gap model results.
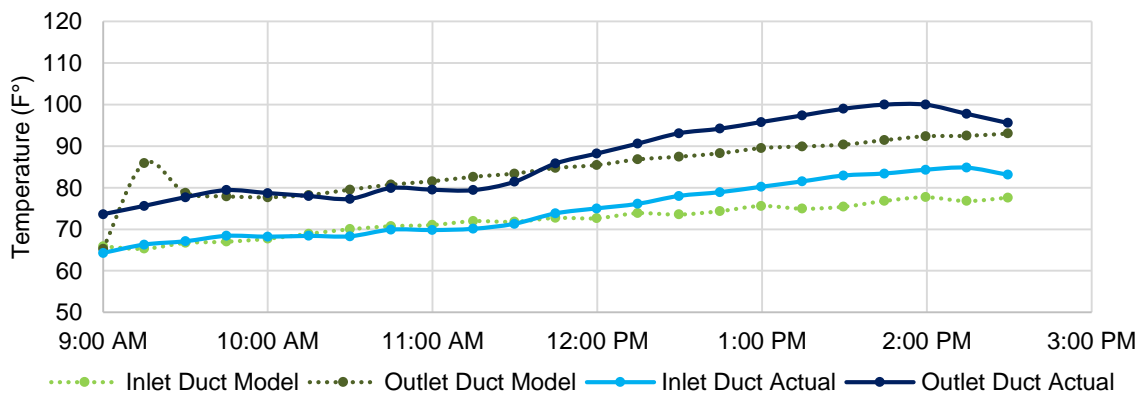

Figure 36. Actual inlet and outlet duct temperature compared to 6inch gap model results.

The simulations of the vented study model agreed well with actual results. Of the three reported simulations, all monitor point temperatures were within 10% of actual. More than 80% of the measurements between the three reported simulations were within 5° F of actual results. The period of time with the most discrepancy was during the conditioning period in the first hour and during hours of high solar insolation.

The vented study was also useful in investigating how the velocity profile in the air gap would compare to the actual scenario. The flow rate and temperature difference of the two ducts can determine how much convective heat is being added to the air before being supplied to the room. Figures 37, 38, and 39 show the hourly simulated air velocity every quarter of an inch between the glazing and the mass wall. The table values of the actual measurements were not accessible but the graphs included in the report provide a good comparison of maximum values and profile (Casperson & Hocevar, 1979, pp. 43-48).
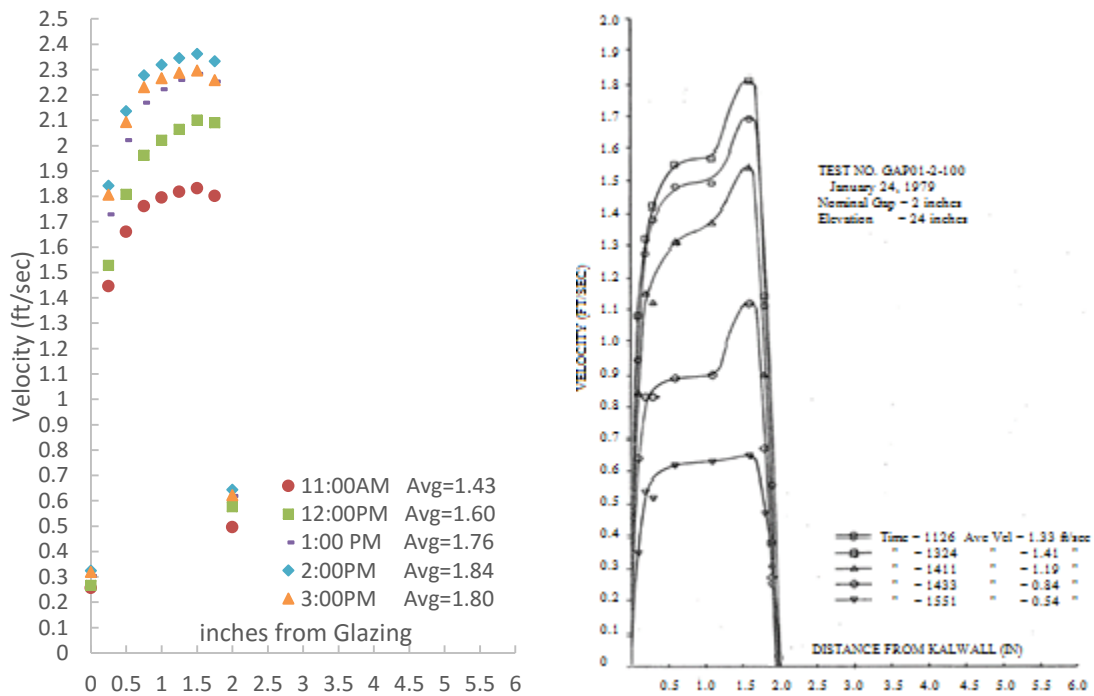

Figure 37. Hourly air velocity profile of 2inch model (left) compared to actual (right).
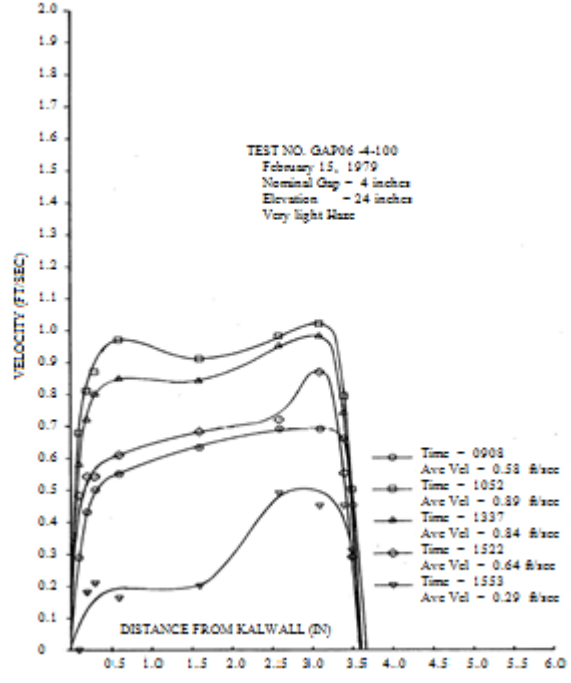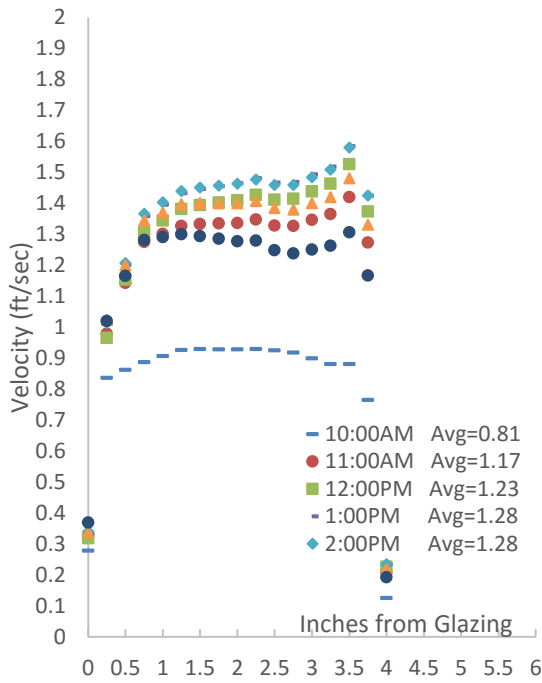
Figure 38. Hourly air velocity profile of 4inch model (left) compared to actual (right).
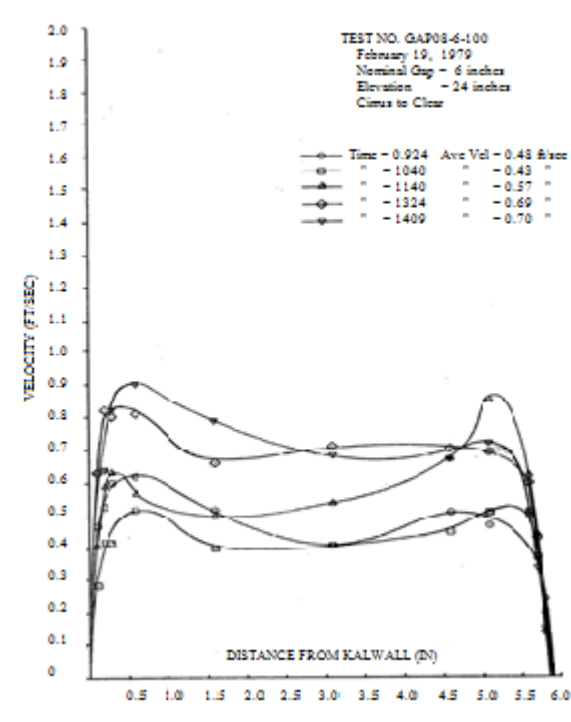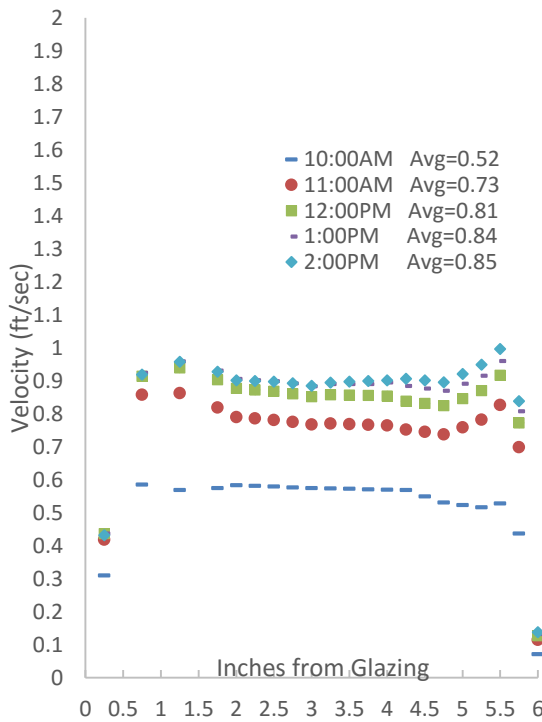

Figure 39. Hourly air velocity profile of 6inch model (left) compared to actual (right).

The sensors were located in the air gap 24 inches above the floor in the center horizontal plane. The velocity profiles act as expected in profile and relationship to one another; however, the model air velocity magnitudes are consistently greater than actual measurements. The difference in modeled air velocity to actual increases as the air gap width decreases. The maximum average velocities are off by 0.41 ft/ sec for the 2 inch gap, 0.39 ft/sec for the 4 inch gap, and 0.15 ft/sec for the 6 inch gap. The flow became more fully developed the further from either surface. High velocity magnitudes are seen closer to the hotter surface mass wall. The relationships between the air gap size and the mximum velocity are cloesly realted. In both the actual and model results the maximum velocity in the 2-inch gap is approximately two times as much as the maximum velocity in the 6 inch gap. The highest magnitudes are when there is the most solar radiation direct on the glazing surface around 1PM and 2PM.

Effects of Numerical Schemes

The number of time steps, iterations, and the size of the mesh can have a large impact on the time of the simulation and the accuracy of the results. The turbulence model chosen would also affect results. An analysis of the different turbulence models on the model results was unable to be done as only the k-epsilon model was able to complete a full simulation. The impact of time step size on results was investigated as an indication of variation caused by user input solving parameters. Autodesk suggests a time step size of 100 seconds for studies involving transient solar radiation over multiple days (*Solar Heating*, 2016). A reference study that looked at time step sensitivity using Autodesk CFD to calculate internal

building temperature showed that the larger the time step size the larger the temperature

fluctuation range (Albatayneh, Alterman, Page, & Moghtaderi, 2015).

The vented 4-inch model was run with three different time step sizes: 900, 300, and

60 seconds. The model used for the time step sensitivity analysis had 7.5 hours of 15-minute

measured data. Results were compared against one another and then to actual data. Results

showed a larger temperature fluctuation with time steps of 900 seconds compared to 300 or

60 seconds. The time it takes for temperatures to stabilize from the initial condition is also

increased with larger time steps. The compared results in Figure 40 show that the run with a

time size of 60 seconds was able to stabilize within the first hour and maintain a tighter range

of temperatures. The 900 second time step did not reach a stabilized state until approximately

1:30 pm with a much larger temperature range.
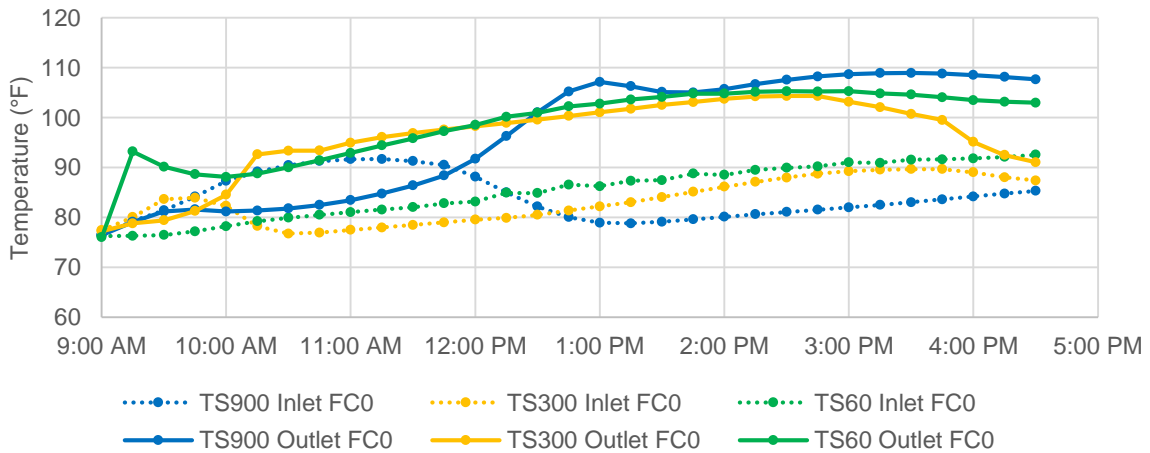
Figure 40. Time step sensitivity results using 4 inch vented model. Time step sizes include
60 seconds, 300 seconds, and 900 seconds.

The results of each time step run were compared to temperature measurements

reported in the vented experimental study (Casperson & Hocevar, 1979). The temperature

difference between modeled inlet and outlet duct temperatures were calculated at 15 minute

intervals. The box plot of Figure 41 shows the range of temperature differences and the average temperature difference for both inlet and outlet sensors for each time step size. The 60 second time step size shows the least temperature difference from actual. Both inlet and outlet averaged below 5° F difference. The increase in temperature fluctuation is with larger time step sizes is depicted well in comparing the increasing range of temperature differences from actual, especially in the outlet temperature measurements.
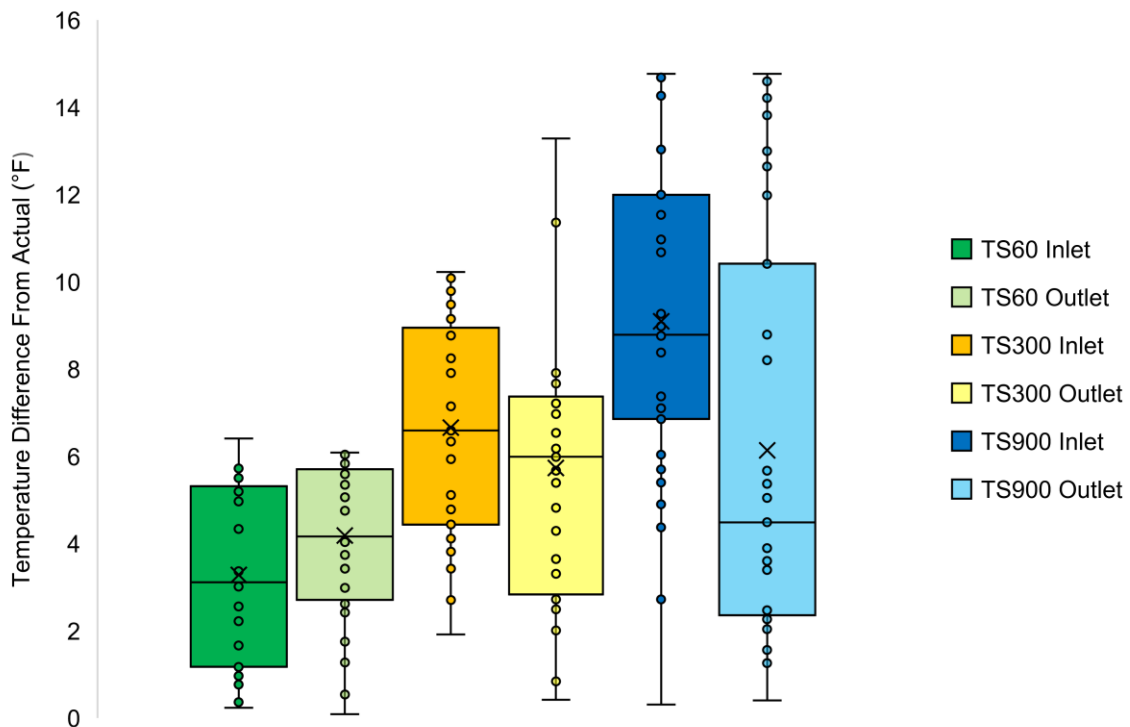
Figure 41. The range and average temperature difference from actual by time step size.

The time step size input has an effect on the accuracy of the model. A smaller time step size may increase results but it also increases the computational time of the simulation. Table 5 lists the time it took to simulate 7.5 hours using time step sizes of 1 minute, 5 minutes, and 15 minutes. The accuracy of each simulation was also listed. The percentage of

model data that was within 5° of actual data for both inlet and outlet temperatures was used

as a measure of simulation accuracy. The simulations were run on an ASUS K501 with a

Dual-Core Pentium CPU @ 2.30 GHz processor with an installed memory (RAM) of 4GB.

Table 5

Results of Time Step Size Sensitivity Listing Computation Time and Accuracy of Simulations Run with Time-step Sizes of 60, 300, and 900 Seconds

Time Step Size (sec)	# of Time Steps	Computation Time	% Inlet Temps within 5° of Actual	% Outlet Temps within 5° of Actual
60	450	4 hours 46 min	68%	58%
300	90	2 hours 10 min	32%	42%
900	30	0 hours 56 min	13%	55%

Chapter Five: Conclusions

The use of computer simulations in building design allows for the designer to better understand and predict the building's performance. The goal of this research was to validate Autodesk CFD for use with Trombe walls by modeling and comparing the results to past experimental studies. A model of both unvented and vented Trombe wall test cells from past experimental studies were created and simulated in Autodesk CFD. The methodology included the creation of geometry, definition of materials, definition of boundary conditions, definition of initial conditions, creation of a mesh, and creation of solving parameters. All steps within the methodology required the interpretation of properties and conditions from the experimental study into the model parameters of the CFD software. Given a digital model, the CFD tool was able to solve for energy, mass, and momentum over the discretized geometry to recreate heat transfer and air flow representing real world conditions.

While this study shows that the accuracy of a model largely depends on the user's ability to operate the software and the availability of good material properties, it also shows that Autodesk CFD can be useful in the analysis of systems like Trombe walls. The visualization of the interior temperature and air flow patterns were as expected and even provided further multi-dimensional information that could prove useful during the early phases of design. The point-to-point comparison did not prove to be accurate within the expected errors of the sensors. The Los Alamos study simulations showed exaggerated temperature fluctuations during the day and night. The vented study model results showed that the CFD tool was able to replicate the air flow and mass wall heat transfer of a Trombe wall to some degree of accuracy.

An analysis was done on the effects of time step durations on model results. The shorter the time step size the longer the computational time and closer to actual results. The mesh refinement also had an effect on computational time but result accuracy was not analyzed in this study. If an equally reasonable result can be reached with longer time steps and coarser mesh, it would decrease the amount of time needed to complete a design study with multiple runs.

While this study may not have accomplished the goal of software validation, a useful framework methodology was created. The continued modeling and validation of passive solar techniques such as Trombe walls using Autodesk CFD or similar CFD tools are suggested to further the adoption of comfort as a performance metric and CFD as a building science tool.

Future Recommendations

There are both short term and long term recommendations stemming from this research. The short term recommendations stem from a recognition of result variability due to user inputs such as time step sizes and mesh definition. This study investigated variation in time step size but it would be beneficial to further define suggested time step sizes for various building analysis purposes. Mesh definition was investigated briefly in this study to find a useful balance between the accuracy of a fine mesh and the quick computation time of a coarse mesh. Further investigation into the effect of mesh sizing on results needs to be completed.

The long term recommendation is for the continued exploration of passive solar building design using computational fluid dynamics. The integration of current building

energy simulation practices with computational fluid dynamic tools requires further research into workflow and validation of indoor environments. Many of the impediments discussed in this paper stemmed from the limited availability of experimental study data. A combined approach, in which the researcher has direct access to the material and sensor data, would enable the researcher to control and account for any uncertainties. A three-dimensional array of both temperature and air velocity sensors installed within the experimental module would enable the researcher to compare to the full capability of a simulated three-dimensional model. The visualization of the simulated results showed a variation in air flow magnitude and temperature within the air gap due to shading that would not be recognized by a single plane of sensors.

Further recommendations into the design of experimental modules for the purpose of validation include varying geometry and materials. Validation of a Trombe wall in a full sized building to understand the extent of the flow and temperature characteristics would be more beneficial to designers. Other passive solar design techniques or even a combination of passive and active systems can be examined using Autodesk CFD. Only masonry Trombe walls were investigated in this study; Trombe walls that incorporate water walls or phase change materials could be analyzed further with a tool specialized for fluid analysis.

Autodesk CFD is a verified product and compatible with design software used in the building industry. This study explored a simplified building workflow from geometry to analysis. A more defined workflow between particular CAD, BIM, BES, and CFD software that can be referenced by design firms would be beneficial to the industry. This workflow could include and analyze the capability to set up and monitor thermal mannequins in Autodesk CFD as a measure of comfort performance. The creation of a design protocol that

gives users a range of suggested inputs and a method of optimization would be helpful to building designers who may not have extensive CFD knowledge. Example inputs would include material properties and sizing of the glazing and thermal storage wall. A method of optimization could be the measured PMV or PPD score of thermal mannequins set up in expected occupied areas. Any simulation tool, when used for building design, requires a great deal of user knowledge and experience. Further research into the use of CFD tools for Trombe wall design will increase user confidence and knowledge.

References

Abdelrahman, M., & ElDabosy, M. (2013). Evaluation of office spaces ventilation using simulation software: El-Dakahlia governmental headquarter as a pilot renovation. *Building Simulation Conference* (pp. 1-8). Cairo: The Egyptian Society of Energy in Buildings and Environmental Design.

Albatayneh, A., Alterman, D., Page, A., & Moghtaderi, B. (2015). The significance of time step size in simulating the thermal performance of buildings. *Advances in Research, 5*(6), 1-12. doi:10.9734/AIR/2015/20223

ASHRAE. (2010). Standard 55: Thermal comfort. In *ASHRAE Handbook.* Atlanta, GA: ASHRAE Inc.

Ault, R., Torcellini, P., & Van Geet, O. (2003). *NREL Wind Site Entrance Building: Design Review and Recommendations.* Oak Ridge, TN: U.S. Department of Energy Office of Scientific and Technical Information.

Balcomb, J. D. (1992). *Passive Solar Buildings.* Cambridge: The MIT Press.

Casperson, R. L., & Hocevar, C. J. (1979). *Experimental investigation of the Trombe wall.* Golden, Colorado: U.S. Department of Energy.

Catalina, T., Virgone, J., & Kuzink, F. (2009). Evaluation of thermal comfort using combined CFD and experimentation study in a test room equipped with a cooling cieling. *Building and Environment*(44), 1740-1750. doi:10.1016/j.buildenv.2008.11.015

Chen, Q. (2009). Ventilation performance prediction for buildings: A method overview and recent applications. *Building and Environment*(44), 848-858. doi:10.1016/j.buildenv.2008.05.025

Chen, Q., & Srebric, J. (2002). A procedure for verification, validation, and reporting of indoor environment CFD analyses. *HVAC & Research, 8*(2), 201-216.

Ellis, P. G. (2003). *Development and validation of the unvented Trombe wall model in EnergyPlus.* Masters Thesis, University of Illinois at Urbana-Champaign, Mechanical Engineering.

Energy Information Administration. (2014). *Annual Energy Review 2014.* Washington D.C.: U.S. Department of Energy. Retrieved from http://www.eia.gov/forecasts/archive/aeo14/

Gan, G. (1998). A parametric study of Trombe walls for pazzive cooling of buildings. *Energy and Buildings*(27), 37-48.

Haupt, S. E., Kunz, R. F., Paltier, L. J., & Dreyer, J. J. (2010). Computational fluid dynamics coupled with thermal impact model for building design. *Journal of Computers, 5*(10), 1552-1559.

Hordeski, M. F. (2004). *Dictionary of energy efficiency technologies.* Lilburn, GA: Fairmont Press.

Kim, S., & Seo, J. (2012). An influence of the opening location of the Trombe wall system on indoor airflow and thermal environment. *ASim* (pp. 34-40). Shanghai: International Building Performance Simulation Association.

Manz, H., & Frank, T. (2005). Thermal simulation of buildings with double-skin facades. *Energy and Building*(37), 1114-1121. doi:10.1016/j.enbuild.2005.06.014

McFarland, R. (1982). *Passive test cell data for the solar laboratory, winter 1980-81.* Solar Energy Group, Los Alamos.

Saadatian, O., Sopian, K., Lim, C., Asim, N., & Sulaiman, M. (2012). Trombe walls: A

    review of oppurtunities and challenges in research and development. *Renewable and*

    Sustainable Energy Reviews(16), 6340-6351. doi:10.1016/j.rser.2012.032

Sami, V. (2003). Applying Computational Fluid Dynamics to Analyze Natural Ventilation &

    Human Comfort in Buildings. *Solar Conference Proceedings* (pp. 851-856).

    American Solar Energy Society.

Sami, V., & Gassman, J. (2006). A simultaneous modelling methodology to analyze passive

    solar performance of Trombe walls. *The 23rd Conference on Passive and Low*

    Energy Architecture. Geneva, Switzerland.

Solar Heating. (2016, March 02). Retrieved from Autodesk CFD 2016:

    https://knowledge.autodesk.com/support/cfd/learn-

    explore/caas/CloudHelp/cloudhelp/2016/ENU/SimCFD-UsersGuide/files/GUID-

    0782555D-8F9D-4A43-A85A-C8F6DBAAA982-htm.html

Thermocouples. (n.d.). Retrieved from Omega:

    http://www.omega.com/prodinfo/thermocouples.html

Torcellini, P., & Pless, S. (2004). Trombe walls in low-energy buildings: Practical

    experiences. *World Renewable Energy Congress VIII* (pp. 1-8). Denver, CO: National

    Renewable Energy Laboratory.

Trombe, F., & Jacques, M. (1972). *U.S. Patent No. 3832992.* Washington, DC: U.S. Patent

    and Trademark Office.

Troubleshooting - Advection Schemes. (2014, January). Retrieved from Autodesk CFD:

    https://knowledge.autodesk.com/support/cfd/troubleshooting/caas/sfdcarticles/sfdcarti

    cles/How-to-choose-an-advection-scheme-in-Autodesk-Simulation-CFD.html

Wilson, A. (1979). *Thermal storage wall design manual.* Albuquerque, NM, USA: New Mexico Solar Energy Association.

Yazdanian, M., & Klems, J. H. (1994). Measurement of the exterior convective film coefficient for windows in low-rise buildings. *ASHRAE Transactions, 100*(1).

Zamora, B., & Kaiser, A. (2009). Thermal and dynamic optimization of the convective flow of Trombe Wall shaped channels by numerical investigation. *Heat and Mass Transfer*(45), 1393-1407. doi:10.1007/s00231-009-0509-6

Zhai, Z. (2006). Application of computational fluid dynamics in building design: Aspects and trends. *Indoor and Built Environment, 15*(4), 305-113. doi:10.1177/1420326X06067336

Vita

Chelsea Renee Davis was born in Itasca, Illinois to Tina Moyer and Craig Davis. She attended public school in Greensboro, NC, and graduated from Walter Hines Page High School. She attended North Carolina State University and majored in Civil Engineering with a minor in Graphic Communications. In May 2014, she graduated Magna Cum Laude with a Bachelor of Science. She enrolled in Appalachian State University in August 2014 as a candidate for a Master of Science degree in Technology, concentrating in Sustainable Design and Construction in the Department of Sustainable Technology and the Built Environment, and graduated in May 2016.